Science of the Total Environment 1054 (2026) 182350

Contents lists available at ScienceDirect

Science of the Total Environment

journal homepage: www.elsevier.com/locate/scitotenv

Species-specific metal handling reveals the decoupling between environmental contamination and biological accumulation in Amazonian mangroves

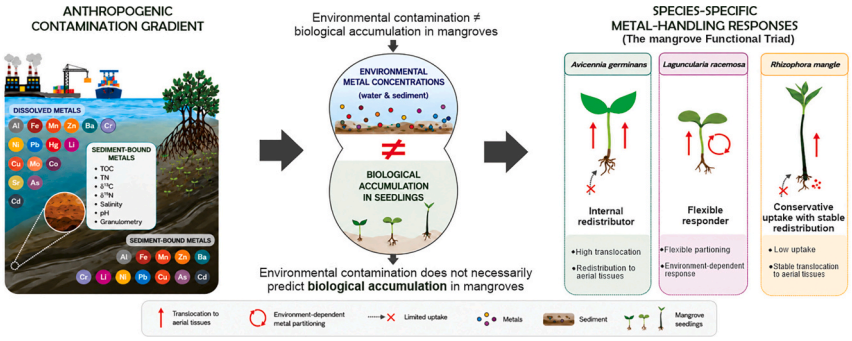
Jacyara Nascimento Corrêa [a,*], Daniel Richard Lemos Brito [b], Ricardo Luvizotto-Santos [b], Carlos Eduardo de Rezende [b,c], Marianna Basso Jorge [a,b,**]

[a] Biodiversity and Biotechnology Network of the Legal Amazon - Rede Bionorte, Universidade Federal do Maranhão, São Luís, MA, Brazil
[b] Graduate Program in Environmental Science and Technology - PPGC&TAmb - Universidade Federal do Maranhão, Cidade Universitária Dom Delgado, Avenida dos Portugueses, n° 1966, 65080-805, São Luís, Maranhão, Brazil
[c] Center for Biosciences and Biotechnology, Environmental Sciences Laboratory, Universidade Estadual do Norte Fluminense Darcy Ribeiro, Avenida Alberto Lamego, n° 2000, 28013-602, Parque Califórnia, Campos dos Goytacazes, Rio de Janeiro, Brazil

HIGHLIGHTS

- Port activities are associated with increased metal contamination in Amazonian estuaries.
- Metal uptake in mangrove seedlings was not directly related to environmental concentrations.
- Species-specific functional responses improved the interpretation of contamination gradients.
- A conceptual Functional Triad framework supports environmental assessment in mangrove systems.

GRAPHICAL ABSTRACT



ARTICLE INFO

Keywords:
Metal handling
Bioindicators
Tropical mangroves
Environmental assessment
Coastal management
Bioaccumulation

ABSTRACT

Environmental assessments of metal contamination in mangrove ecosystems are commonly based on environmental concentrations, although these measurements do not necessarily reflect biological accumulation. Here, we investigated how sediment geochemistry and species-specific metal handling, encompassing metal uptake, retention/partitioning, and translocation, are associated with biological accumulation in mangrove seedlings growing along a gradient of port influence on the Brazilian Amazon coast. Metals were quantified in water, sediments, and seedlings of three dominant mangrove species across six sites representing contrasting levels of anthropogenic disturbance, together with sediment geochemical characterization (TOC, TN, $\delta^{13}C$, and $\delta^{15}N$). Contamination indices indicated higher metal contamination at sites influenced by port activities (PLI > 1, I_{geo} class 2, and C_{deg} up to 17.6). However, metal accumulation in seedlings did not consistently follow environmental contamination gradients. Instead, accumulation patterns varied among species and were associated with

* Corresponding author.
** Correspondence to: M.B. Jorge, Biodiversity and Biotechnology Network of the Legal Amazon - Rede Bionorte, Universidade Federal do Maranhão, São Luís, MA, Brazil.
E-mail addresses: jacyaranc@gmail.com (J.N. Corrêa), mb.jorge@ufma.br (M.B. Jorge).

https://doi.org/10.1016/j.scitotenv.2026.182350
Received 23 July 2026; Received in revised form 24 September 2026; Accepted 7 October 2026
Available online 15 October 2026
0048-9697/© 2026 The Authors. Published by Elsevier B.V. This is an open access article under the CC BY license (http://creativecommons.org/licenses/by/4.0/).
The Article Processing Charge for the publication of this research was funded by the Coordenação de Aperfeiçoamento de Pessoal de Nível Superior - Brasil (CAPES) (ROR identifier: 00x0ma614).

differences in sediment geochemistry and metal-handling responses. *Avicennia germinans* predominantly translocated metals to aerial tissues, *Laguncularia racemosa* exhibited context-dependent shifts between retention and translocation, whereas *Rhizophora mangle* maintained comparatively stable redistribution patterns. These contrasting responses indicate that biological accumulation cannot be inferred solely from environmental metal concentrations and highlight the importance of species-specific physiological responses for interpreting contamination patterns. Collectively, our findings support the Functional Triad as a conceptual framework based on correlative patterns in which sediment geochemistry, inferred metal availability, and species-specific metal handling interact to shape patterns of biological accumulation in mangrove ecosystems. This integrative perspective provides a basis for improving the interpretation of contamination gradients and may contribute to the development of biologically informed environmental assessment approaches for tropical mangroves.

1. Introduction

Metal contamination resulting from industrial, urban, and port activities represents a significant threat to coastal ecosystems, particularly in mangrove environments where metals accumulate in estuarine waters and sediments, with potential impacts on biological communities (Chen et al., 2023; Li et al., 2022). While essential metals (e.g., Cu, Fe, Mn, Li, and Zn) act as micronutrients at low concentrations, non-essential metals (e.g., Ag, Al, Cd, Pb, and Hg) are toxic even at trace levels (Zhang et al., 2023; Briffa et al., 2020). Mangroves function as key biogeochemical barriers, where fine sediments and organic matter promote metal sequestration and retention within the ecosystem. As a result, mangroves act both as long-term sinks and as potential secondary sources of contamination through biological uptake (Szafranski and Granek, 2023; Nubi et al., 2022; Hossain et al., 2020).

The distribution and bioavailability of metals in mangrove ecosystems are controlled by sediment properties, including grain size, total organic carbon (TOC), total nitrogen (TN), C/N ratio, phosphorus, sulfur, and stable isotopes ($\delta^{13}C$, $\delta^{15}N$). These parameters are widely used as tracers of organic matter provenance and anthropogenic influence (Jatobá-Junior et al., 2025; Nascimento et al., 2025; Mziray and Kimirei, 2024; Sartori et al., 2023; Carneiro et al., 2021). Beyond their role as geochemical indicators, these physicochemical characteristics also influence biological processes in mangrove systems, as sediment contamination and geochemical conditions can affect plant physiology and growth (Alhassan and Aljahdali, 2021; Das et al., 2019). At the same time, vegetation actively modifies sediment chemistry, nutrient cycling, and metal-binding capacity, creating feedback mechanisms that further regulate metal dynamics (Chanda et al., 2021; Chai et al., 2019).

Mangrove species possess specialized physiological mechanisms for metal ion regulation, including uptake, translocation, and detoxification processes, which contribute to their tolerance to metal exposure. These mechanisms underpin functional responses to metal exposure, reflected in species-specific patterns of metal accumulation and internal redistribution (Rahman et al., 2024; Hossain et al., 2022). Such patterns provide a basis for linking sediment contamination to plant physiological responses and broader ecosystem conditions. Accordingly, mangroves have been widely recognized as effective biological indicators for pollution assessment in tropical coastal environments (Alam et al., 2022; Bakshi et al., 2018). Furthermore, mangrove seedlings provide an opportunity to investigate metal uptake and internal redistribution during early developmental stages, when environmental exposure may influence establishment and subsequent plant development. However, metal-handling responses in seedlings may differ from those observed in mature trees, which should be considered when extrapolating the findings across developmental stages.

Considering their ecological and biogeochemical roles, assessing contamination in mangroves is essential for environmental management. Brazil holds the second-largest mangrove area globally, with the Amazon coast containing the largest continuous mangrove forest (Souza Filho, 2005). This study focuses on the Maranhense Gulf in northern Brazil, encompassing the São Marcos (SMEC) and São José (SJEC) estuarine complexes. The region is influenced by the São Luís Port Terminal Complex (CPSL), with port and industrial activities concentrated around the SMEC. These contrasting levels of anthropogenic influence provide a suitable gradient for investigating relationships between environmental contamination and biological accumulation in mangrove ecosystems.

Previous studies have documented metal contamination in water, sediments, crabs, fish, and macroalgae in this region (Macedo et al., 2024; Corrêa et al., 2023; Righi et al., 2022; Jesus et al., 2021; Delgado et al., 2020; Carvalho-Neta et al., 2019). However, an integrated assessment of metal bioaccumulation and handling by mangrove plants remains poorly resolved along the Amazon coast. We hypothesize that mangrove species exhibit distinct metal-handling responses, rather than acting solely as passive sinks, and that differences in sediment geochemistry may modulate metal availability and contribute to contrasting patterns of biological accumulation. We further hypothesize that integrating environmental metal concentrations, sediment geochemical characteristics, and species-specific uptake, translocation, and accumulation patterns may provide a conceptual basis for interpreting contamination gradients beyond traditional concentration-based approaches.

This study aims to: (1) assess metal contamination and identify its sources in sediments, water, and mangrove seedlings across two estuarine complexes with contrasting degrees of port influence; (2) characterize species-specific metal handling responses in *Avicennia germinans*, *Laguncularia racemosa*, and *Rhizophora mangle*; and (3) develop a conceptual framework of species-specific metal-handling responses (Functional Triad) to support the interpretation of contamination gradients in mangrove systems. From an environmental monitoring perspective, understanding how mangrove species respond to contamination gradients is essential for improving assessment frameworks in coastal systems. Traditional approaches based solely on chemical concentrations may not fully explain patterns of biological accumulation. The integration of sediment geochemistry with biological responses supports the conceptual framework proposed in this study and highlights the importance of species-specific metal handling for interpreting contamination dynamics in tropical mangrove ecosystems.

2. Materials and methods

2.1. Study area

To assess the effects of anthropogenic influence, six sampling sites were selected across two estuarine complexes on the Brazilian Amazon coast (Fig. 1). Four sites (P1–P4) were located within the São Marcos Estuarine Complex (SMEC), directly influenced by the São Luís Port Terminal Complex and associated industrial activities, urban sewage discharge, agricultural runoff, and pesticide inputs. Two additional sites (P5 and P6) were located in the São José Estuarine Complex (SJEC), representing areas with lower port influence, characterized by extensive mangrove forests, artisanal fisheries, ecotourism activities, and surrounding agricultural areas. Detailed information on sampling sites, including coordinates and associated anthropogenic activities, is provided in Supplementary Table S1. This sampling design enabled the assessment of an anthropogenic disturbance gradient between port-affected and less-impacted mangroves. The region is characterized by

a semidiurnal macrotidal regime with high-energy tidal currents (Santos et al., 2020). The climate presents marked seasonality, with a rainy period (January–June) and a dry period (August–December) (NUGEO, 2016).

2.2. Sampling and processing of water, sediment, and mangrove samples

Surface and interstitial water salinity, as well as surface pH, were measured in situ using calibrated probes. Surface water samples were collected in duplicate at depths <0.5 m. Sampling was conducted in June 2023, at the end of the rainy season. For dissolved metal analysis, samples were filtered (0.45 μm), acidified with high-purity nitric acid (HNO_3, pH < 2, Suprapur® Merck), and refrigerated until analysis.

Duplicate surface sediment samples were collected at each sampling site using a spatula, immediately refrigerated, and subsequently lyophilized (L101 Liotop®). The dried material was used for grain-size distribution, metal quantification, and elemental and isotopic analyses.

A total of ten seedlings per species (n = 10 per species per site, *A. germinans*, *L. racemosa*, *R. mangle*) were collected at each site, except for *R. mangle* at site P3, where the species was absent. Each seedling was processed individually to assess intraspecific variability in metal accumulation. These species were selected based on their dominance in the study area and their relevance for environmental assessment. In the laboratory, seedlings were washed with deionized water, separated into roots, stems, and leaves, dried at 60 °C to constant mass, ground, and stored for analysis (Chowdhury et al., 2023).

2.3. Grain size distribution, elemental (C and N) and isotopic ($\delta^{13}C$ and $\delta^{15}N$) analysis of sediment

Sediment grain-size distribution (< 2 mm) was determined by laser diffraction (Shimadzu SALD-3101), without removal of carbonates or organic matter. No chemical pretreatment was applied, so the measured particle-size distribution reflects the sediment in its natural composition. Particles were classified as sand, silt, or clay according to the Wentworth scale. Certified standards were used to determine particle size distribution, and the accuracy found was 96%.

Elemental (C and N) and stable isotopic compositions ($\delta^{13}C$ and $\delta^{15}N$) were determined to characterize organic matter sources and early diagenetic processes (Rezende et al., 1990). Analyses followed Sartori et al. (2023), using a Thermo Scientific Flash 2000 EA coupled to a Delta V Advantage IRMS (Thermo Scientific). Total carbon (TC) and total nitrogen (TN) were measured directly. For total organic carbon (TOC), samples were treated with 2 M HCl to remove inorganic carbon before analysis. Analytical control was performed for every 10 samples using certified isotopic standards (Elemental Microanalysis Protein Standard OAS: 46.5 ± 0.78% for C; 13.32 ± 0.40% for N; − 26.98 ± 0.13 ‰ for $\delta^{13}C$; + 5.94 ± 0.08 ‰ for $\delta^{15}N$) and analytical uncertainties were determined (0.05% for OC, 0.03% for N, and ± 0.2 ‰ for $\delta^{15}N$ and $\delta^{13}C$). Analytical accuracy exceeded 95%.

Isotopic values are reported relative to Pee Dee Belemnite ($\delta^{13}C$) and atmospheric nitrogen ($\delta^{15}N$), expressed using standard delta notation: δX (‰) = [(R_sample / R_standard) − 1] × 1000, where X represents $\delta^{13}C$ or $\delta^{15}N$, and R is the ratio of heavy to light isotopes ($^{13}C/^{12}C$ or $^{15}N/^{14}N$).

2.4. Acid digestion and quantification of major and minor elements

Water samples were digested according to USEPA method 3015 A (USEPA, 2007) and Sartori et al. (2023). Sediment samples (~0.5 g dry weight) were digested following a modified USEPA 3052 protocol (USEPA, 1996), using a closed-vessel microwave system with 13 mL of aqua regia (HCl 37% + HNO_3 65%, 3:1 *v*/v) at 180 °C for 40 min. Extracts were filtered and diluted to 35 mL with 0.5 M HNO_3.

Plant tissues (~0.1 g dry weight) were digested with 8 mL of aqua regia, pre-incubated overnight at room temperature, and subsequently processed in a microwave system for 25 min (Pestana et al., 2019). After cooling, extracts were filtered and diluted to 15 mL with 0.5 M HNO_3.

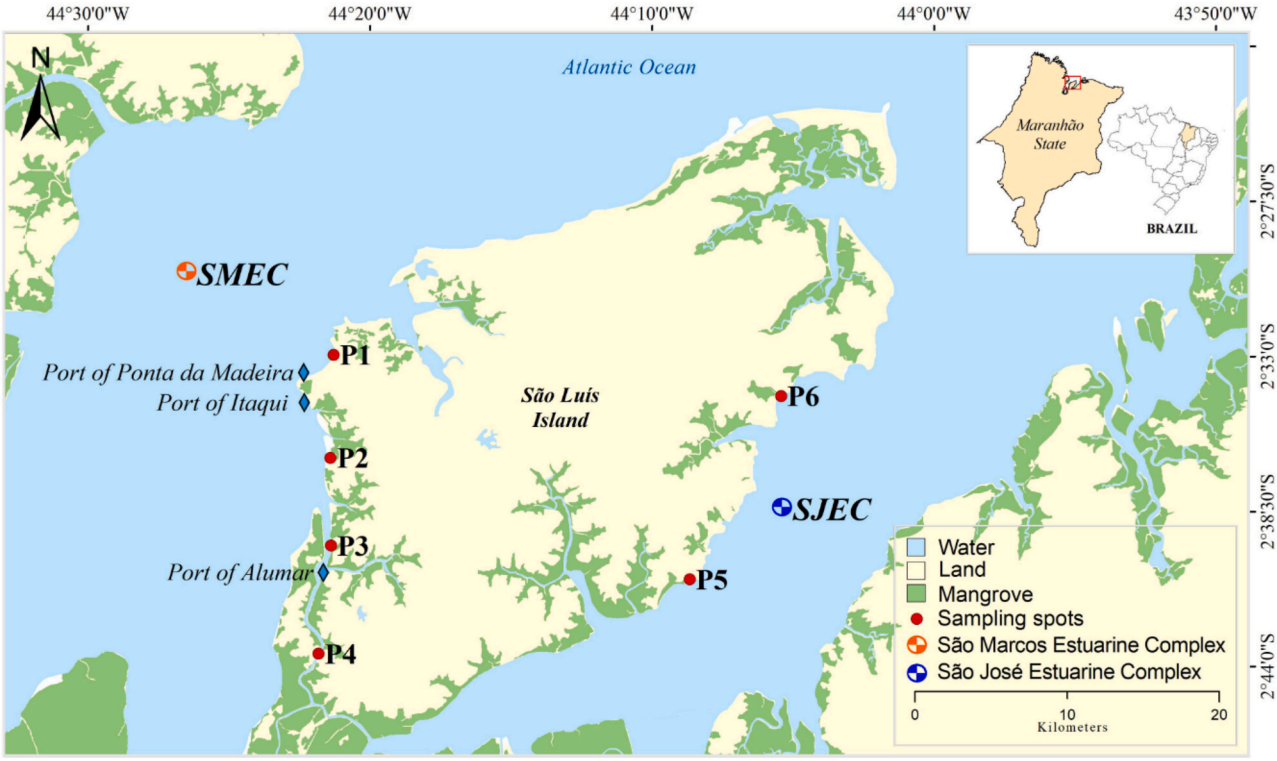


Fig. 1. Location of sampling sites in the São Marcos Estuarine Complex (SMEC; P1–P4) and São José Estuarine Complex (SJEC; P5 and P6) along the Brazilian Amazon coast.

Element concentrations were determined using Inductively Coupled Plasma Mass Spectrometry (ICP-MS; Agilent 7850, Agilent Technologies, USA). Procedural blanks and analytical duplicates were included for quality control. Analytical accuracy was verified using certified reference materials (NIST 1646a and NIST 1515), with recoveries ranging from 80% to 120%.

2.5. Indices for assessing metal contamination and functional responses

Environmental indices were applied to evaluate contamination levels, ecological risk, and potential pollution sources. Equations and classification criteria are provided in Table S2 (see Supplementary Material). Water quality was assessed using the Metal Pollution Index (MPI), while sediment quality was evaluated using the Contamination Factor (Cf), Contamination Degree (C_{deg}), Pollution Load Index (PLI), Geoaccumulation Index (I_{geo}), Enrichment Factor (EF), Potential Ecological Risk Factor (ERI), and the Ecological Risk Index (RI). Metal availability was interpreted based on measured metal concentrations in water and sediments in conjunction with sediment geochemical characteristics, rather than directly quantified through chemical speciation.

Results were compared with Sediment Quality Guidelines (NOAA) and Brazilian regulations (CONAMA 357/2005 for water and 454/2012 for sediment). Biological implications were interpreted using Threshold Effect Levels (TEL), Probable Effect Levels (PEL), Effects Range-Low (ERL), and Effects Range-Median (ERM).

Functional responses of mangrove species were evaluated using the Bioconcentration Factor (BCF), Bioaccumulation Factor (BAF), and Translocation Factor (TF). Two bioconcentration factors were calculated: BCF_{sed}, based on total sediment concentrations, and BCF_{wat}, based on dissolved metal concentrations. These indices were evaluated separately to characterize plant–sediment and plant–water relationships. The BAF was calculated from the metal concentrations measured in stems and leaves relative to the corresponding environmental compartment (sediment or water), using the arithmetic mean of the available stem/environment and leaf/environment ratios to represent shoot-level accumulation. The TF was calculated as the ratio between shoot and root concentrations. Species were classified as excluders (BCF/BAF < 1), indicators (BCF/BAF $= 1$), or accumulators (BCF/BAF > 1) (Baker, 1981).

The percentage of samples exceeding sediment quality guidelines (SQGs) was calculated for each metal using TEL, PEL, ERL, and ERM thresholds, with CONAMA Levels 1 and 2 evaluated separately across all sampling sites.

2.6. Statistical analysis

Data normality and homogeneity of variances were assessed using the Shapiro–Wilk and Levene tests, respectively. As assumptions for parametric tests were not met, Kruskal–Wallis tests were applied to evaluate overall differences among sites and species.

Multivariate analyses included hierarchical cluster analysis (HCA), performed using the Unweighted Pair Group Method with Arithmetic Mean (UPGMA) and Bray–Curtis similarity, and principal component analysis (PCA) was applied to sediment variables to explore relationships among sampling sites. Before PCA, variables were standardized to account for differences in measurement scales. Kaiser normalization was applied, and principal loadings were used for the biplot with standardized scores. All analyses were conducted using R (v4.1.2), PAST (v4.17),

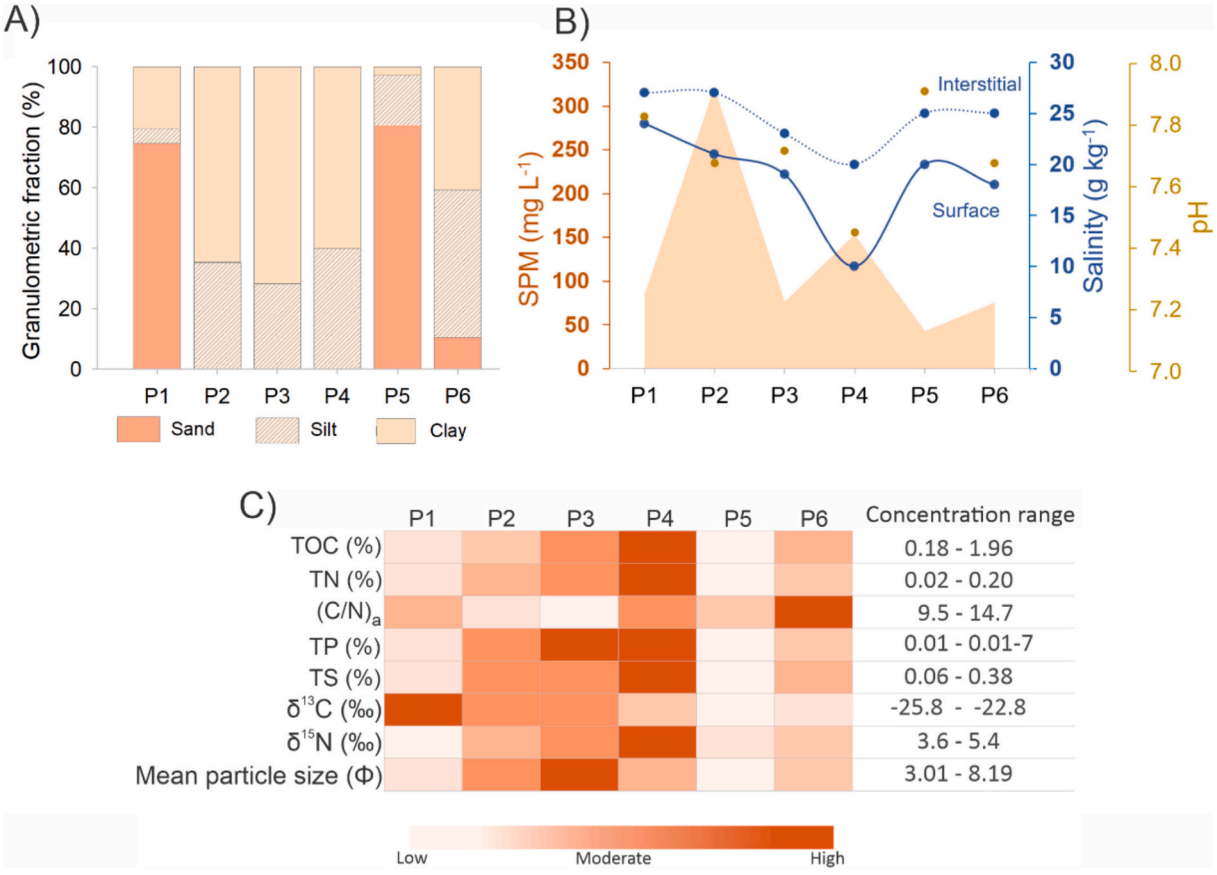


Fig. 2. (A) Distribution of sediment grain-size classes. (B) Physicochemical parameters of surface and interstitial water. (C) Geochemical parameters of surface sediments at mangrove sampling sites in the São Marcos Estuarine Complex (SMEC; P1–P4) and the São José Estuarine Complex (SJEC; P5–P6). Abbreviations: TOC, total organic carbon; TN, total nitrogen; C/N, atomic carbon-to-nitrogen ratio; TP, total phosphorus; TS, total sulfur; $\delta^{13}C_{org}$, stable carbon isotope ratio of organic matter; $\delta^{15}N_{total}$, stable nitrogen isotope ratio of total sediment.

Jamovi (v2.7) and SigmaPlot (v14.5).

3. Results

3.1. Sediment and water characteristics

Sediments across the study area were predominantly muddy, with sand dominating only at sites P1 and P5 (74.4 and 80.7%, respectively) (Fig. 2A). Surface water salinity ranged from 10 (P4) to 24 g kg^{-1} (P1), whereas interstitial salinity varied between 20 (P2) and 27 g kg^{-1}(P1). Surface water pH remained relatively stable, ranging from 7.4 (P4) to 7.9 (P5). Suspended particulate matter (SPM) was highest at P2 (321 mg L^{-1}) and lowest at P5 (43 mg L^{-1}) (Fig. 2B).

Geochemical parameters of surface sediments are presented in Fig. 2C. TOC and TN concentrations were higher at SMEC sites (P2–P4), reaching 1.96 and 0.20%, respectively, whereas the lowest values were recorded at P5 (0.18 and 0.02%). The C/N ratio ranged from 9.5 (P3) to 14.7 (P6). $\delta^{13}C_{org}$ values were more negative at SJEC sites (−25.8 ‰ at P5; −25.2 ‰ at P6) compared to SMEC (−22.8 ‰ at P1). In contrast, $\delta^{15}N_{total}$ values were higher at SMEC sites (5.1 ‰ at P2, 5.3 ‰ at P3, and 5.4 ‰ at P4). Total phosphorus (TP) and total sulfur (TS) reached maximum values at P4 (735.9 and 3797.5 mg kg^{-1}, respectively).

3.2. Metal concentrations in water, sediment, and indices

Dissolved metal concentrations exhibited clear spatial variation among sampling sites (Fig. 3A). Overall, dissolved metal concentrations were higher in the SMEC, particularly P2–P4, where several elements reached their maximum values, including Al (853 µg L^{-1}) and Fe (883 µg L^{-1}) at P2 and Ba (30 µg L^{-1}) at P4. In contrast, sites within the SJEC

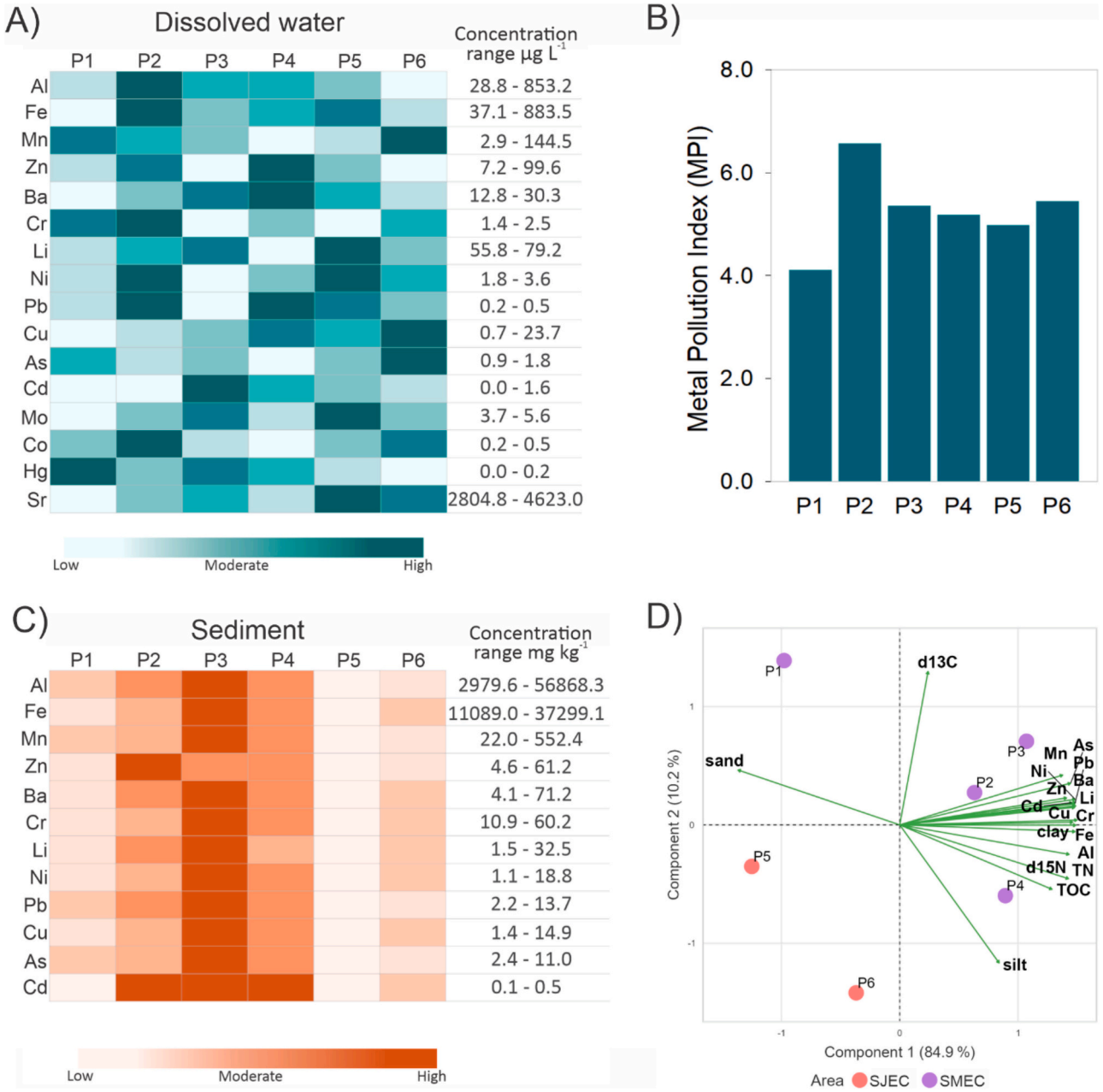


Fig. 3. (A) Heatmap of dissolved metal concentrations in water (µg L^{-1}). (B) Metal Pollution Index (MPI). (C) Metal concentrations in surface sediments (mg kg^{-1} dry weight). (D) Principal Component Analysis (PCA) based on the correlation matrix, showing the distribution of sampling sites and environmental variables in the São Marcos Estuarine Complex (SMEC; P1–P4) and the São José Estuarine Complex (SJEC; P5–P6).

generally exhibited lower concentrations. However, localized increases were observed, with P5 showing higher values for Sr, Mo, Ni, and Li, and P6 for Mn, Cu, and As.

The MPI followed a similar spatial pattern, reaching its highest value at P2 (Fig. 3B), indicating elevated overall contamination at this site. Hierarchical Cluster Analysis (Fig. S1A) segregated sampling sites according to total metal load and grouped elements into four assemblages based on likely sources: G1 (Hg, Co, Pb, Cd), G2 (Cr, As, Mo, Ni, Cu), G3

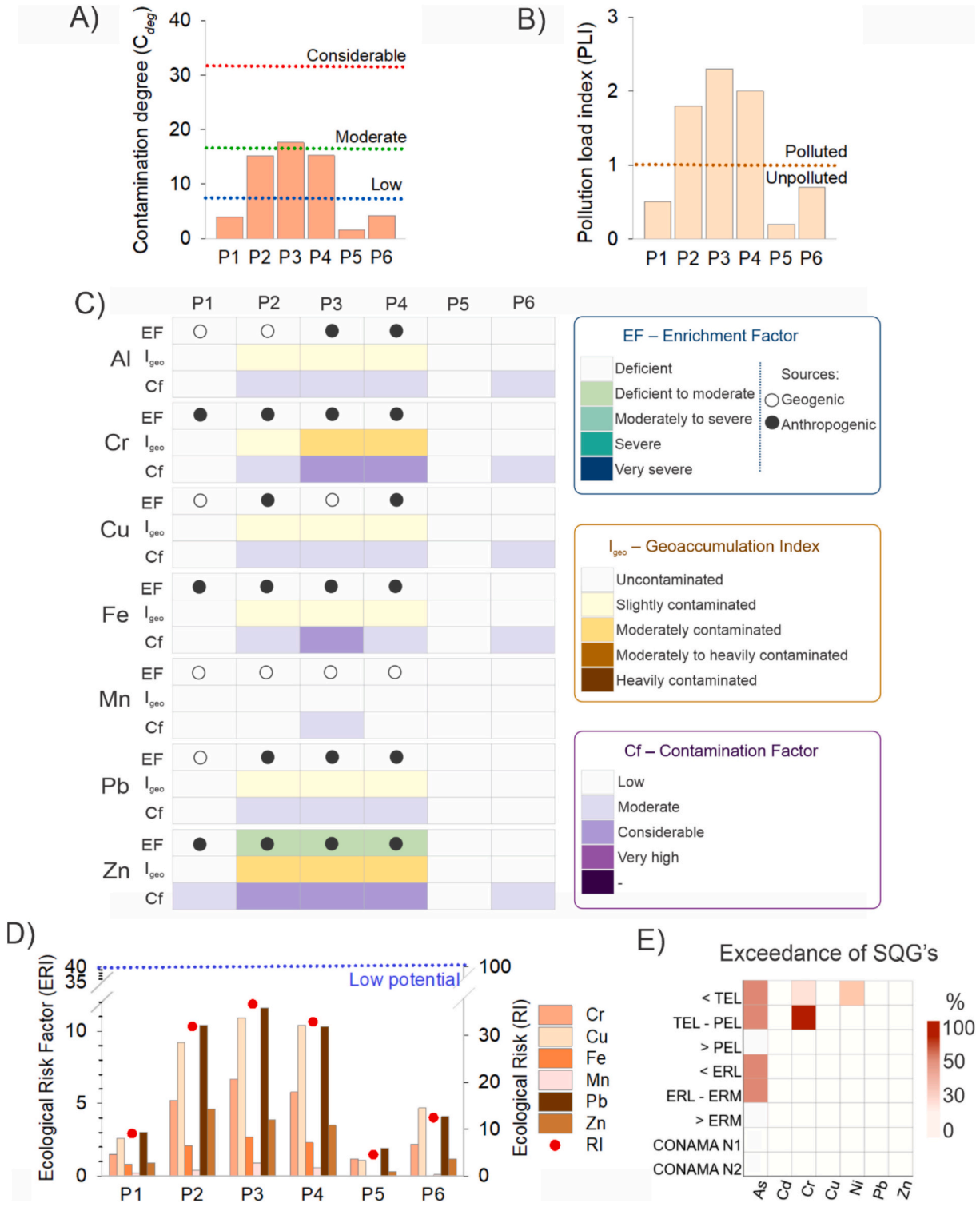


Fig. 4. Indices for surface sediments at mangrove sampling sites in the São Marcos Estuarine Complex (SMEC; P1–P4) and the São José Estuarine Complex (SJEC; P5–P6). (A) Contamination Degree Index (C_{deg}). (B) Pollution Load Index (PLI). (C) Enrichment Factor (EF), Geoaccumulation Index (I_{geo}), and Contamination Factor (Cf). (D) Ecological Risk Factor (ERI) and Potential Ecological Risk Index (RI). (E) Percentage of samples exceeding sediment quality guidelines (SQGs) for selected metals in mangrove sediments. Values represent the proportion (%) of samples exceeding the TEL-PEL, ERL and ERM sediment quality guideline thresholds, with exceedances of CONAMA Level 1 (N1) and Level 2 (N2) evaluated separately. SQG thresholds were based on NOAA criteria (Long et al., 1995) and CONAMA guidelines. Percentages were calculated considering all sampling sites ($n = 6$) for each metal.

(Mn, Li, Zn, Ba, Al, Fe), and G4 (Sr). These assemblages indicate distinct geochemical behaviors and potential sources, with G1 elements associated with anthropogenic inputs, whereas G3 reflects mixed lithogenic and anthropogenic contributions.

Sedimentary metal concentrations (Fig. 3C) followed the order: Al > Fe > Mn > Ba > Cr > Zn > Li > Ni > Cu > Pb > As > Cd, with higher concentrations generally occurring at P2–P4. Principal Component Analysis (Fig. 3D) explained 84.9% of the total variance along PC1, while PC2 explained an additional 10.25%, accounting for 95.11% cumulatively. PC1 clearly separated sandy sites (P1 and P5) from muddy, organic-rich sites (P2, P3, P4, and P6). Most metals (Al, As, Cd, Cr, Cu, Fe, Li, Mn, Ni, Pb, Zn) showed positive loadings on PC1, with particularly strong loadings for Cu (0.9992), Fe (0.9930), Li (0.9923), Ba (0.9902), Ni (0.9888), Pb (0.9870), Cr (0.9863), Al (0.9882), and Cd (0.9718). Clay (0.9750) and TN (0.9544) also showed strong positive loadings, whereas sand showed a strong negative loading (−0.9116), supporting the separation of sandy and finer-textured sites. PC2 was mainly associated with $\delta^{13}C_{org}$ (0.8646) and silt (−0.7783). The complete PCA loadings are provided in Supplementary Material, Fig. S2. PCA scores showed that P1 and P5 occupied negative positions along PC1, whereas P2, P3, and P4 showed positive PC1 scores. P6 occupied an intermediate position along PC1 (−0.3682) but had the most negative PC2 score (−1.4196). This position was aligned with the strong negative loading of silt on PC2 (−0.7783) and opposed to the positive loading of δ^{13}Corg (0.8646), rather than being associated with elevated metal concentrations (Supplementary Material, Fig. S2). These patterns indicate that the position of P6 in the multivariate space was associated with sediment characteristics represented by PC1 and PC2, rather than by metal concentrations alone.

Cluster analysis (Fig. S1B) grouped sites into three clusters: G1 (P6), G2 (P1 and P5), and G3 (P2, P3, and P4), while metals were organized into five assemblages: G1 (Al, Fe), G2 (As, Ni, Pb, Cu), G3 (Zn, Cr, Ba, Li), G4 (Mn), and G5 (Cd). These clustering patterns are consistent with PCA results, reinforcing the separation between sediment types and highlighting the role of sediment properties in controlling metal distribution.

Contamination indices (Fig. 4) varied among sampling sites. The C_{deg} ranged from 1.6 (P5) to 17.6 (P3) (Fig. 4A). The PLI exceeded 1.0 at sites P2, P3, and P4, with a maximum of 2.3 at P3, whereas SJEC sites remained close to background conditions (Fig. 4B).

Zinc showed the highest enrichment, with I_{geo} values up to 1.6 at P2, Cf of 4.6, and EF >1.5 at P2, P3, and P4 (Fig. 4C). Chromium and Fe also showed EF >1.5 at multiple sites, indicating enrichment relative to background levels. In contrast, Al, Cu, Pb, and Mn presented EF <1.5 at most locations.

Ecological risk indices (ERI and RI) were below 40 and 150, respectively, for all elements (Fig. 4D). The percentage of samples exceeding sediment quality guidelines was calculated for each metal using TEL, PEL, ERL, and ERM thresholds, with CONAMA Levels 1 and 2 evaluated separately across all sampling sites. Comparison with sediment quality guidelines (Fig. 4E; Table S3) showed that As, Cr, and Ni exceeded TEL in part of the samples. Arsenic concentration was below TEL in 50% of the samples and fell within the ERL–ERM range in the remaining samples. Cd, Cu, Pb, and Zn remained below TEL and ERL values. All concentrations were within limits established by CONAMA Resolution 454/2012.

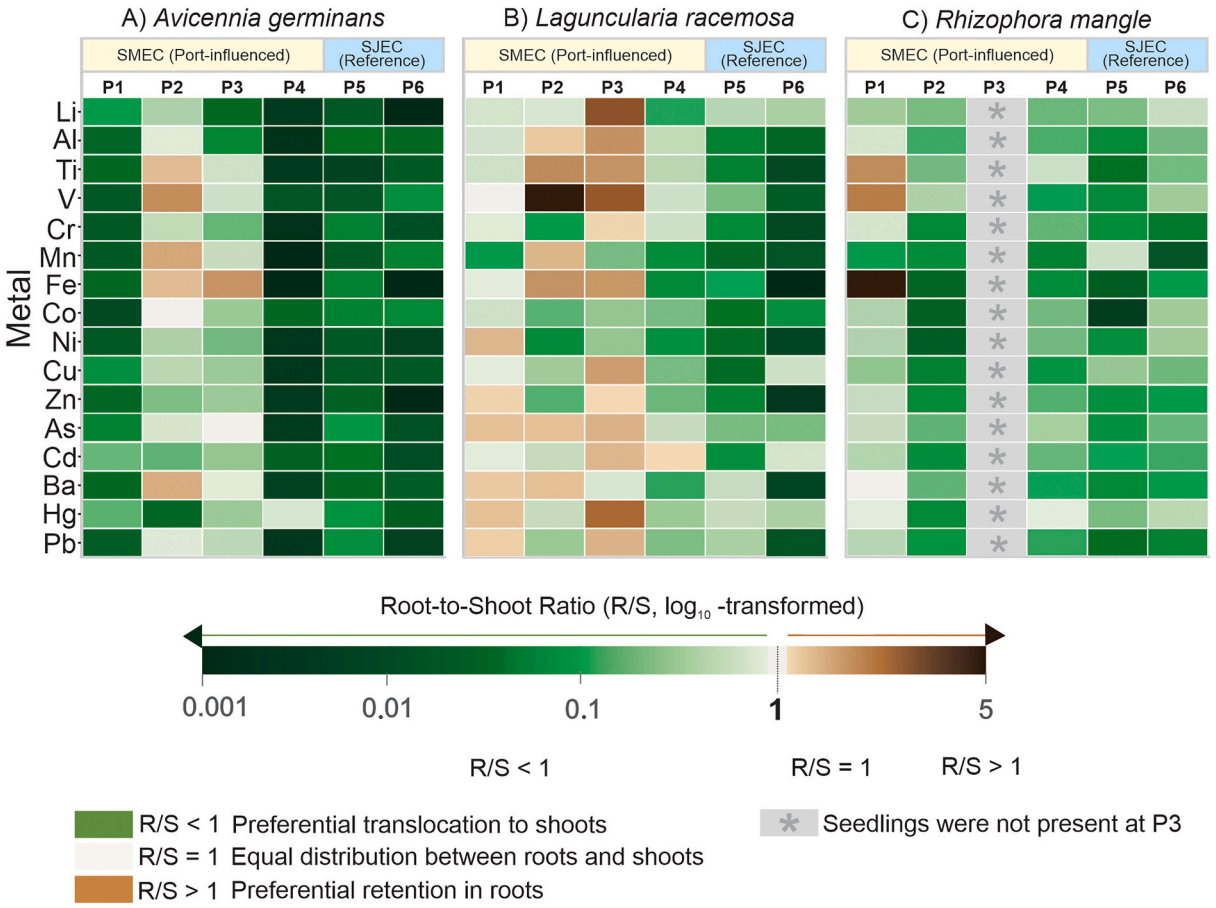


Fig. 5. Root-to-shoot ratio (R/S, $\log_{10}$ - transformed) of metals in the mangrove species *Avicennia germinans* (A), *Laguncularia racemosa* (B), and *Rhizophora mangle* (C) at sampling sites in the São Marcos Estuarine Complex (SMEC; P1–P4) and the São José Estuarine Complex (SJEC; P5–P6). The asterisk (*) indicates that seedlings were not present at P3.

3.3. Metal accumulation patterns in mangrove seedlings

Metal concentrations in mangrove seedlings varied across species, sites, and plant tissues, reflecting differences in environmental exposure and species-specific physiological responses (Fig. 5 and Table S4). At P3, *R. mangle* seedlings were not encountered at the sampling location and, therefore, no tissue concentration data were available for this species at this site. The overall metal burden followed the order *A. germinans* > *L. racemosa* > *R. mangle* in the SMEC, and L. *racemosa* > *A. germinans* > *R. mangle* in the SJEC.

A. germinans generally exhibited higher concentrations in shoots than roots, indicating a predominance of metal accumulation in aerial tissues. In contrast, *L. racemosa* displayed greater spatial variability, with higher concentrations in roots at SMEC sites and a more balanced distribution between tissues in the SJEC. Site P6 was distinguished by the highest Li concentrations observed in the study and a predominance of shoot accumulation. *R. mangle* showed the lowest overall metal burden and a comparatively stable accumulation pattern, with relatively small differences between tissues, although some elements exhibited localized root enrichment at specific sites.

3.4. Evaluation of functional responses to metal contamination

The TF revealed species- and site-specific patterns of metal allocation (Fig. 6). *A. germinans* exhibited high variability, with a predominance of translocation (TF >1), particularly at sites P4 and P6, and root retention restricted to specific elements at P2 and P3. *L. racemosa* showed a site-dependent pattern, characterized by root retention at port-influenced SMEC sites and a shift toward translocation at SJEC sites, with maximum values observed at P6. *R. mangle* displayed a predominantly translocation-oriented behavior across most sites, with occasional element-specific deviations indicating localized variation in internal metal allocation.

The BCF_{sed} values were generally below 1.0, indicating a predominant excluder strategy across species (Fig. 6). Instances of $BCF_{sed} > 1$ were limited and restricted to specific elements and sites, particularly in *A. germinans* and L. *racemosa*, while *R. mangle* exhibited $BCF_{sed} < 1$, consistent with an excluder strategy under the studied conditions. In contrast, BCF_{wat} values showed greater variability, suggesting a stronger influence of the dissolved phase. *A. germinans* exhibited a transition from excluder behavior at most sites to localized accumulation at P2 and P6. *L. racemosa* displayed a broader shift toward accumulation at intermediate and less impacted sites, while *R. mangle* maintained a predominantly excluder behavior, with accumulation restricted to specific elements at P4.

The BAF_{sed} values were mostly below 1.0, indicating limited accumulation in aerial tissues relative to sediment concentrations, with few exceptions at specific sites (Fig. 6). In contrast, BAF_{wat} exhibited mixed patterns, with both exclusion and accumulation depending on species and site conditions. *A. germinans* showed alternating behavior across sites, *L. racemosa* exhibited a consistent shift toward accumulation under less impacted conditions, and *R. mangle* maintained predominantly excluder behavior with localized increases in aerial accumulation.

Overall, BCF_{sed} and BCF_{wat} did not always provide consistent interpretations across species and sampling sites, with contrasting patterns evident when BCF_{sed} was <1 while BCF_{wat} was >1 (Fig. 6). These differences, together with the observed BAF patterns, followed variation in sediment geochemistry and metal partitioning between dissolved and sediment-associated fractions.

3.5. Integration of functional patterns: The functional triad

The integration of TF, BCF, and BAF revealed three complementary functional responses to metal exposure across the studied estuarine gradient. While environmental contamination was generally higher at port-influenced sites, species responses were not directly proportional to metal concentrations, indicating the influence of sediment geochemistry and species-specific physiological traits.

A. germinans was characterized by a predominantly translocation-oriented response, *L. racemosa* exhibited flexible shifts between root retention and translocation according to site conditions, and *R. mangle* displayed a more stable pattern characterized by regulated uptake and redistribution.

Together, these complementary responses are synthesized in the Functional Triad proposed in this study (Fig. 7), which summarizes the dominant species-specific patterns of metal handling observed across the contamination gradient. This conceptual framework integrates uptake, accumulation, and translocation patterns to describe how mangrove species respond to metal exposure under contrasting environmental conditions. Rather than representing discrete categories, the Functional Triad reflects a continuum of functional responses modulated by sediment geochemistry, metal availability, and anthropogenic influence, based on the correlative patterns observed in this study.

4. Discussion

4.1. Water and sediment contamination: Sources, geochemical controls, and management implications

Spatial patterns of dissolved metals reflected differences between the two estuarine complexes. In the SMEC, elevated Al and Fe at site P2 coincided with the highest SPM values observed in the study, suggesting an association with sediment resuspension processes, such as dredging. This pattern is consistent with observations reported for port-influenced systems (Cutrim et al., 2025). The exceedance of regulatory thresholds (CONAMA 357/, 2005) at this site indicates localized increases in Al, Fe, and Cu concentrations. These results reinforce the relevance of monitoring sediment resuspension processes in port environments.

In the SJEC, elevated concentrations of Sr, Mo, Ni, Li, Mn, Cu, and As at sites P5 and P6 are consistent with inputs associated with diffuse sources, such as urban runoff and domestic effluents (Haydous et al., 2025; Thanh-Nho et al., 2018). Hierarchical clustering revealed distinct metal assemblages (G1–G4), reflecting similarities in behavior or potential sources. For example, the grouping of Hg, Co, Pb, and Cd (G1) is commonly associated with anthropogenic inputs, whereas Mn, Li, Zn, Ba, Al, and Fe (G3) are often linked to mixed geogenic and anthropogenic influences. This spatial variability provides evidence for multiple metal sources across the study area.

In macrotidal estuaries, seasonal hydrology and tidal variability may influence dissolved metal concentrations, SPM dynamics, and biological exposure. These processes can promote sediment resuspension and modify the partitioning of metals between dissolved and particulate phases, potentially affecting their transport and uptake by organisms (Thanh-Nho et al., 2018; Santos et al., 2020; Niu et al., 2021; Correa et al., 2025). Along the Amazonian Equatorial Coast, seasonal and spatial differences in water-quality conditions have also been associated with metal bioaccumulation in mangrove oysters (Correa et al., 2025). Because water sampling in the present study was conducted during low tide, the measured dissolved metal and SPM concentrations represent conditions at this tidal stage and do not capture variability across the tidal cycle.

Sedimentary geochemistry indicates that metal retention is associated with organic matter dynamics. Higher TOC and TN values at SMEC sites are consistent with inputs related to port activities, while elevated TOC at P6 may reflect contributions from stream-derived material. C/N ratios and $\delta^{13}C_{org}$ values indicate mixed organic matter sources, including terrestrial and marine inputs (Carneiro et al., 2021; Meyers, 1997). Enriched $\delta^{15}N$ values at SMEC sites are consistent with nitrogen inputs commonly associated with anthropogenic sources, such as sewage or agricultural runoff (Yadav et al., 2025; Liu et al., 2020).

The observed geochemical conditions, including elevated TS and TP, are consistent with sulfate reduction processes in reducing

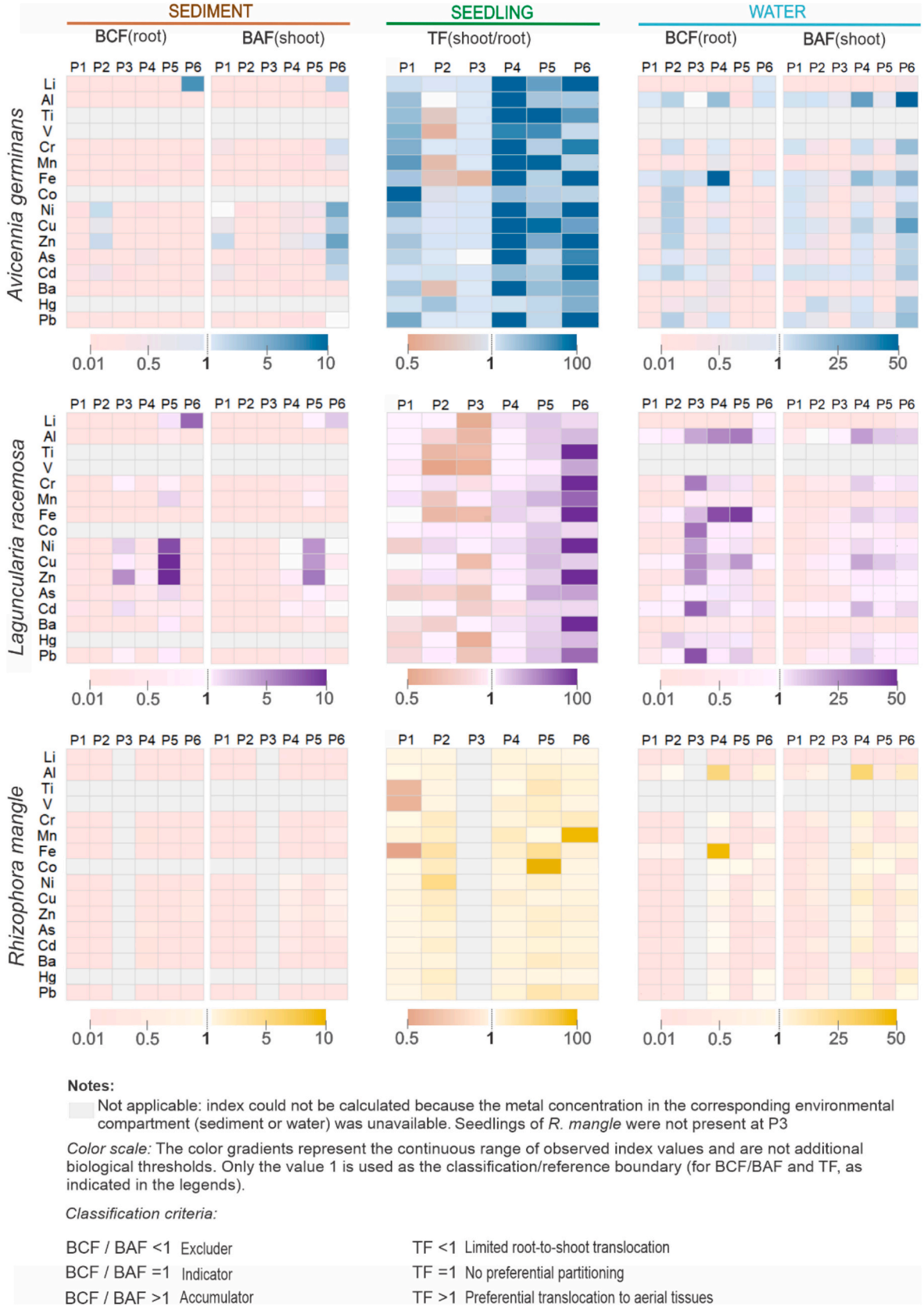


Fig. 6. Bioconcentration Factor (BCF), Bioaccumulation Factor (BAF), and Translocation Factor (TF) calculated for mangrove seedlings in relation to sediment and water concentrations at sampling sites in the São Marcos Estuarine Complex (SMEC; P1–P4) and the São José Estuarine Complex (SJEC; P5–P6).

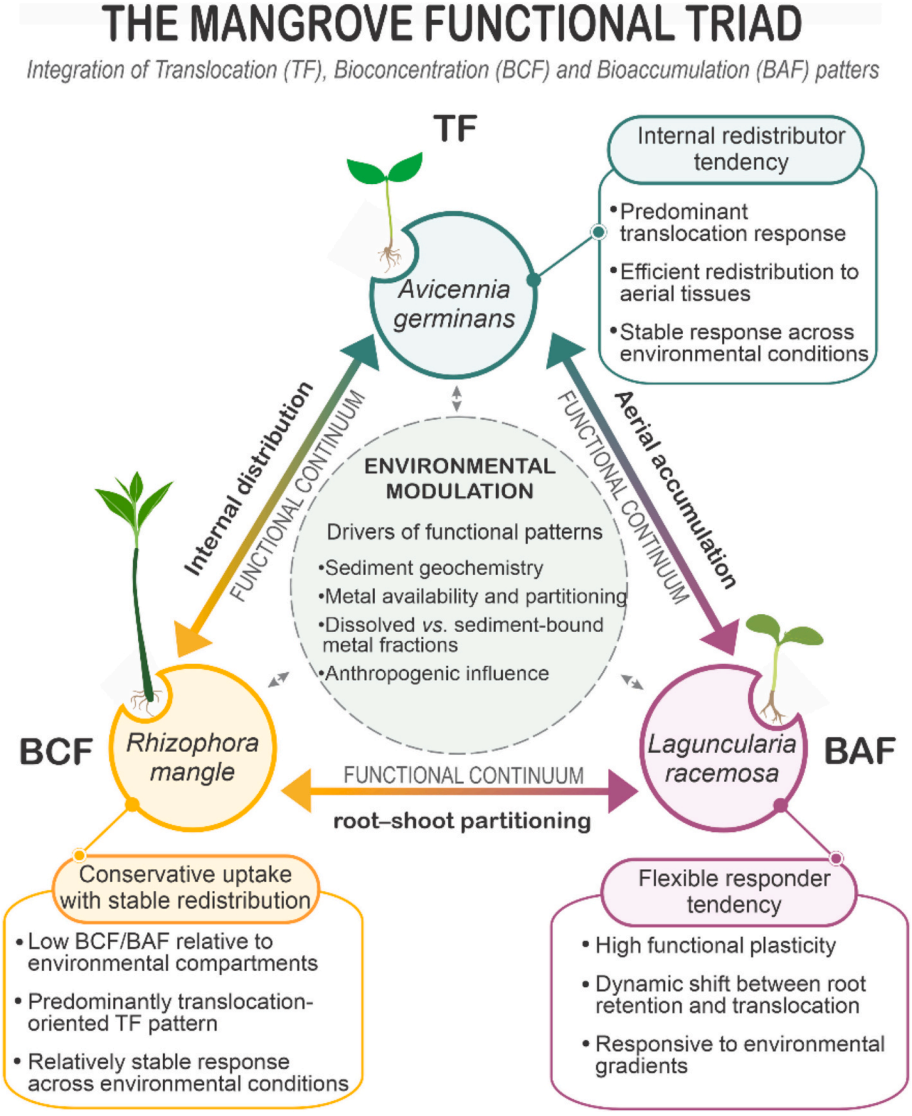


Fig. 7. Summary of the species-specific metal-handling patterns observed across the studied estuarine gradient. The Functional Triad synthesizes the dominant patterns of uptake, translocation, and accumulation observed in the three mangrove species. *Avicennia germinans* exhibited a predominantly translocation-oriented response, *Laguncularia racemosa* displayed environmentally modulated shifts between root retention and translocation, and *Rhizophora mangle* showed a comparatively stable pattern characterized by low accumulation relative to environmental compartments and predominantly translocation-oriented internal redistribution. These patterns are interpreted in the context of sediment geochemistry, inferred metal availability, and anthropogenic influence, within a conceptual framework based on correlative patterns rather than mechanistically validated processes. The positions of the species represent dominant tendencies along a functional continuum rather than fixed categories, and may shift according to environmental conditions.

environments. Under these conditions, metals may be immobilized as sulfides, limiting mobility and bioavailability (Costa et al., 2020; Lacerda et al., 1991). This context helps explain why metal uptake by mangrove seedlings did not directly reflect total sediment concentrations. These observations indicate that assessments based solely on total metal concentrations may not fully explain patterns of biological accumulation because availability may be influenced by sediment geochemistry.

Multivariate analyses indicate that metal distribution is associated with sediment texture and organic matter content. Cluster analysis separated port-influenced sites (P2–P4) from less impacted areas. Metal groupings suggest differences in origin and behavior; for example, Al—Fe is commonly associated with lithogenic sources, whereas As–Ni–Pb–Cu and Zn–Cr–Ba–Li groupings are consistent with anthropogenic inputs or post-depositional processes (Ashayeri et al., 2023). These patterns support the interpretation of mixed geogenic and anthropogenic contributions.

Contamination indices indicated variation among sites, with higher values at SMEC locations. Elevated PLI (>1.0) values at these sites are consistent with increased contamination levels, while SJEC sites showed values closer to background conditions. Element-specific indices (e.g., Cf and EF) indicated variability among metals, with Zn, Cr, and Fe showing higher enrichment relative to other elements. These responses are consistent with contributions from both anthropogenic and natural sources.

A discrepancy was observed between contamination indices and ecological risk indices. While some indices indicated elevated contamination, RI values suggested low ecological risk. This contrast has also been reported in other mangrove systems (Islam et al., 2026) and may reflect limitations of index-based approaches. Previous ecotoxicological studies in the region report biological effects despite similar index values (Silva et al., 2023; Righi et al., 2022; Jesus et al., 2021; Carvalho-Neta et al., 2017, 2019). These observations suggest that integrating biological responses may improve the interpretation of ecological risk.

Comparison with SQGs indicates that As, Cr, and Ni exceeded threshold values in a portion of the samples. Arsenic exceeded TEL in 50% of samples but remained below PEL. Although other metals remained below threshold values, the presence of As above guideline levels suggests potential ecotoxicological relevance. These results complement national regulatory assessments (CONAMA 454/, 2012).

4.2. Metal accumulation patterns in mangrove seedlings

Metal accumulation patterns in mangrove seedlings varied among species and sites, reflecting interactions between environmental conditions and species-specific responses. In the SMEC, the overall metal burden followed the order *A. germinans* > *L. racemosa* > *R. mangle*, whereas in the SJEC, *L. racemosa* exhibited the highest accumulation. These differences are consistent with a contribution of local environmental conditions, including sediment characteristics, to patterns of metal uptake (Sreelekshmi et al., 2022).

Distinct accumulation patterns were observed among species. *A. germinans* generally showed greater accumulation in aerial tissues, whereas L. *racemosa* displayed marked spatial variability, including elevated Li concentrations at P6. *R. mangle* exhibited lower overall accumulation, although its highest metal burden was also recorded at P6, one of the sites least influenced by port activities.

The interpretation of tissue metal concentrations in the present study is constrained by the limited availability of phytotoxicity thresholds specifically established for mangrove seedlings. Values reported for adult trees, other mangrove species, or terrestrial crops may provide useful context, but cannot be directly transferred to the seedlings and tissues evaluated here because metal tolerance may vary with species, developmental stage, organ, and exposure conditions. Although several metals, including Cu, Zn, Pb, and As, were detected in the tissues, suitable tissue-specific phytotoxicity thresholds for mangrove seedlings are not available for quantitative comparison. This lack of species- and tissue-specific thresholds represents an important knowledge gap and should be considered when interpreting the tissue metal concentrations reported in this study.

Across species, variations in metal concentrations were not directly proportional to environmental contamination levels. Sites with lower apparent anthropogenic influence occasionally showed elevated metal accumulation, suggesting that sediment geochemistry and inferred metal availability may play a more important role in plant uptake than total environmental concentrations alone (Donaher et al., 2024; Rezaei et al., 2021). This pattern was particularly evident at P6, where elevated accumulation occurred despite lower influence from port-related activities. These observations are consistent with a potential contribution of sediment geochemistry, together with contamination intensity, to patterns of metal accumulation in mangrove seedlings. Consequently, accumulation patterns should be interpreted in the context of local environmental conditions and species-specific physiological regulation rather than as direct proxies of environmental contamination.

4.3. Mechanisms of metal uptake, retention, and translocation

Metal uptake and internal redistribution in mangrove seedlings appear to be associated with the interaction between sediment geochemistry, inferred metal availability, and species-specific physiological traits rather than reflecting environmental concentrations alone (MacFarlane et al., 2007; Rahman et al., 2024). Fine sediments enriched in organic matter and sulfur promote metal complexation and sulfide formation, reducing the availability of sediment-bound metals despite elevated total concentrations (Abeywardhana et al., 2022). Consequently, differences in metal accumulation among species are better interpreted as functional responses consistent with differences in metal available pools than as passive reflections of contamination levels (MacFarlane et al., 2007; Rahman et al., 2024). These observations help explain the decoupling observed between environmental concentrations and plant accumulation across sampling sites, which in this study refers to a non-linear spatial relationship rather than temporal process. Because apoplastic barriers, symplastic transport, radial oxygen loss, and salt gland activity were not directly measured, these processes are considered here as literature-supported hypotheses that may help explain the observed accumulation and translocation patterns, rather than as mechanisms demonstrated by the present study.

4.3.1. General patterns of metal uptake and exclusion

The predominantly low BCF_{sed} and BAF_{sed} values (<1) indicate limited transfer of metals from sediments to plant tissues. This pattern is consistent with both reduced metal availability in mangrove sediments and processes that favor root retention over internal redistribution (Suman et al., 2018; El-Sharkawy et al., 2025). This decoupling between total sediment concentrations and plant uptake has been reported in mangroves (Rezaei et al., 2021; Karmakar et al., 2025) and other wetland halophytes (Donaher et al., 2024). Lead (Pb) exemplifies this pattern, as its consistently low BCF values indicate limited transfer from sediments to plant tissues despite moderate sediment concentrations (Usman et al., 2013).

In contrast, BCF_{wat} and BAF_{wat} values were more variable, with several instances exceeding unity, indicating accumulation relative to the measured dissolved metal concentrations (Zhou et al., 2022). However, BCF_{wat} values derived from point measurements of dissolved metals may be sensitive to tidal variability and should therefore be interpreted within the tidal conditions of sampling. This compartment-specific behavior highlights an important functional distinction: while mangroves tend to exclude sediment-bound metals, they may selectively accumulate elements from the water column, potentially influencing water quality even when sediment-associated contamination remains relatively stable (Lacerda et al., 2022, 2024).

This apparent excluder response is consistent with root-level barriers that have been reported to limit uptake and upward transport in mangroves (Rahman et al., 2024; Yan et al., 2017), although such mechanisms were not directly assessed in the present study. These processes may contribute to metal retention under anoxic, reducing sediment conditions, where metal availability may be constrained by geochemical processes (Abeywardhana et al., 2022; Usman et al., 2013; MacFarlane et al., 2007). In some species, particularly within the *Avicennia genus*, rhizosphere modification through radial oxygen loss may locally enhance metal bioavailability (Abeywardhana et al., 2022; Lewis et al., 2011), underscoring the complexity of plant–sediment interactions.

Despite generally low BCF and BAF values, TF data revealed active internal redistribution processes. The combination of TF >1 and low BCF is consistent with preferential translocation of absorbed metals to aerial tissues, rather than necessarily indicating enhanced uptake capacity (Hossain et al., 2022; Suman et al., 2018). This pattern highlights the importance of internal metal partitioning in shaping species-specific translocation responses (Bhargava et al., 2012). Recent community-level evidence also indicates that metal allocation may differ among organs, with root-to-stem transfer exceeding root-to-leaf translocation for most elements and with biochemical traits related to stress resistance contributing to metal retention in roots and stems (Du et al., 2026). This comparison supports the interpretation that the TF patterns observed in the present study may reflect differential internal partitioning rather than uniformly enhanced uptake. However, the biochemical traits and transport pathways identified by Du et al. (2026) were not measured here and should therefore be considered possible explanatory mechanisms rather than mechanisms demonstrated by the present study.

The predominance of low BCF and BAF values observed in the present study is consistent with the sediment geochemistry of the investigated estuaries. Higher contents of organic matter, sulfur and fine particles at SMEC may favor metal complexation and sulfide precipitation, potentially reducing metal availability despite elevated total concentrations. Therefore, the local geochemical setting may contribute to differences in inferred metal availability, while species-specific

physiological mechanisms may contribute to differences in uptake, retention, and translocation patterns, consistent with previous studies in mangrove sediments (MacFarlane et al., 2007; Abeywardhana et al., 2022).

4.3.2. Species-specific functional responses

Species-specific responses further highlight distinct responses of metal handling. *A. germinans* exhibited consistently high translocation capacity, particularly at sites P4 and P6, as indicated by TF values >1. Despite this efficient internal redistribution, metal concentrations in plant tissues generally remained lower than those measured in sediments for most elements, resulting in BCF_{sed} values <1. Similar responses have been reported for *A. marina*, which shows TF >1 for Cu and Zn despite low BCF values (Kumari and Pathak, 2025; Rezaei et al., 2021), and for *A. officinalis*, characterized by BCF <1 coupled with TF >1 (Hossain et al., 2022).

If metals are retained in the aerial tissues of *A. germinans*, they may be released into the mangrove detrital pool through leaf senescence and litter decomposition. This process could create a potential exposure pathway for detritivores and other consumers, particularly because metal accumulation has been documented in the muscle tissue of the mangrove crab *Ucides cordatus* in Amazonian mangroves (Jesus et al., 2021). However, because metal transfer from mangrove tissues to consumers was not evaluated in the present study, the potential contribution of *A. germinans* litter to trophic exposure should be regarded as a hypothesis requiring direct investigation.

TF values >1 for several non-essential metals (e.g., Li, Al, Ti, As, Cd, Ba, Hg, and Pb) indicate preferential allocation to aerial tissues, a pattern consistent with mechanisms of metal regulation reported for mangrove species (Rahman et al., 2024) and with observations in *Acanthus ilicifolius* showing extreme Pb translocation (Siregar et al., 2025). Similar patterns have been discussed in the context of root-level exclusion processes and other responses previously reported for mangroves (Rahman et al., 2024; Yan et al., 2017). In Avicennia species, salt gland activity has been proposed as one possible contributor to ion regulation and, indirectly, to metal accumulation patterns (Ding et al., 2024; Guo et al., 2023; MacFarlane et al., 2007). However, its contribution to the metal translocation patterns observed here was not directly evaluated. Similar patterns have been reported for *A. schaueriana*, which showed high Fe accumulation in aerial tissues (Arrivabene et al., 2016).

The predominance of translocation in *A. germinans* may therefore reflect efficient internal redistribution under the environmental conditions of the study area. This interpretation is consistent with physiological regulation reported for *Avicennia* species, including salt and ion regulation, but the contribution of salt glands or specific transport pathways was not directly assessed in the present study (MacFarlane et al., 2007; Guo et al., 2023; Rahman et al., 2024). Thus, the coexistence of low BCF values and high TF values supports a pattern of internal redistribution, whereas these mechanisms were not directly assessed in the present study.

In contrast, *L. racemosa* exhibited a site-dependent response. At SMEC sites, which showed the highest contamination indices within the study area, root retention predominated (TF <1), indicating restricted translocation and reduced exposure of aerial tissues (Yan et al., 2017). At SJEC sites, however, a shift toward translocation (TF >1) was observed, suggesting greater redistribution under less impacted conditions. This transition, also reported for Fe in L. *racemosa* by Arrivabene et al. (2016), may be associated with differences in salinity, redox conditions, and organic matter content, which have been reported to influence metal availability in mangrove sediments (Bakshi et al., 2018; Aljahdali and Alhassan, 2020). These environmental factors provide a plausible context for the observed shift, whereas the apparent environmental plasticity of L. *racemosa* may involve changes in root retention and redistribution of absorbed metals to aerial tissues under contrasting site conditions (Arrivabene et al., 2016; Yan et al., 2017). The physiological basis of this apparent plasticity remains to be tested experimentally.

The elevated Li accumulation at P6 is consistent with a potential contribution of local geochemical conditions to the observed accumulation pattern, highlighting the sensitivity of L. *racemosa* to environmentally driven variation in metal availability. This context-dependent behavior contrasts with the more stable responses observed in *A. germinans* and *R. mangle*, suggesting that environmental conditions may contribute to variation in shaping species-specific metal handling responses (Abeywardhana et al., 2022).

R. mangle exhibited a predominantly translocation-oriented profile, with TF >1 for most metals, indicating a predominance of internal redistribution. Similar patterns of translocation of some non-essential metals have been reported for mangroves (Rahman et al., 2024). However, localized reductions in translocation (e.g., Ti, V, Fe, and Ba at P1) indicate that this pattern was not uniform across all elements and sites. Rather than indicating low physiological responsiveness, the relatively stable behavior of *R. mangle* suggests a comparatively consistent pattern of metal handling across contrasting environmental conditions. The limited variation in translocation observed among sites indicates that internal redistribution may be less influenced by local environmental variability than in L. *racemosa*, although the physiological mechanisms underlying this stability remain poorly understood (Rahman et al., 2024). This interpretation concerns the stability of the observed TF patterns and should not be taken as evidence for a specific transport or exclusion mechanism.

Metal-specific regulation was particularly evident for Fe, for which *R. mangle* has been shown to restrict translocation under elevated concentrations (Arrivabene et al., 2016), a pattern consistent with processes limiting Fe redistribution reported in previous studies (Rahman et al., 2024; Yan et al., 2017). These findings indicate that translocation patterns vary among metals, suggesting selective regulation of internal redistribution.

Among the three species, *L. racemosa* provided the clearest evidence that metal handling responses can be environmentally modulated rather than representing fixed species traits. The transition from root retention under higher contamination levels to increased translocation under less impacted conditions is consistent with environmentally modulated metal partitioning and may indicate physiological plasticity. However, the mechanisms underlying this response were not directly assessed in the present study. This context-dependent response suggests that shifts in translocation patterns may serve as sensitive indicators of changes in sediment geochemistry and inferred metal availability before substantial differences become evident from concentration-based assessments alone. Therefore, *L. racemosa* emerges as a promising candidate for future studies investigating environmentally driven variation in metal handling responses across tropical mangrove ecosystems.

Taken together, these complementary species-specific responses indicate that mangrove metal handling cannot be adequately described by a single accumulation strategy. Instead, the observed patterns support the interpretation that species-specific metal handling reflects complementary physiological responses across contrasting environmental conditions.

4.4. Implications, limitations, and future perspectives of the functional triad

The complementary functional responses documented in this study highlight functional differences in metal handling among mangrove species, addressing a recognized limitation in these systems, where root retention often predominates over internal redistribution (Yadav et al., 2023; Liu et al., 2024). The integration of species with distinct functional traits broadens the range of responses observed, combining sediment stabilization and metal translocation across varying contamination conditions. Within this context, the proposed conceptual framework brings together these complementary responses, supporting the interpretation of contamination gradients in mangrove ecosystems by

linking sediment properties with biological responses.

A. germinans exhibited a predominance of metal translocation across sites, whereas L. *racemosa* showed a site-dependent pattern, while *R. mangle* displayed a more consistent translocation profile. Collectively, these species-specific responses form the basis of the proposed Functional Triad, representing complementary functional roles rather than discrete remediation responses. This conceptual framework proposed here describes environmentally modulated responses along a functional continuum, rather than discrete species-level categories, emerging from the interaction between sediment geochemistry, inferred metal availability, and species-specific physiological regulation. In this context, "functional" refers to the ecological role that each species performs in regulating metal uptake, retention, and redistribution under contrasting environmental conditions.

The observed patterns are consistent with environmentally modulated responses associated with the local geochemical setting and associated environmental gradients, rather than fixed species-level behaviors. Within the context of the studied system, the conceptual framework provides a useful perspective for interpreting metal dynamics, while its applicability to other tropical mangrove ecosystems remains to be evaluated. Although developed using three dominant Amazonian mangrove species, the conceptual framework proposed here should be considered a regional working hypothesis requiring validation across other tropical mangrove systems.

From an ecological interpretation perspective, the Functional Triad proposed here links sediment geochemistry with species-specific biological responses, providing an additional perspective for understanding contamination gradients (MacFarlane et al., 2007; Rahman et al., 2024). Rather than replacing conventional contamination indices, which primarily describe environmental exposure, the Functional Triad incorporates species-specific patterns of metal uptake, accumulation, and translocation, adding a biological dimension to the interpretation of contamination gradients. This perspective is particularly relevant in mangrove sediments, where organic matter content and redox-controlled sulfide formation strongly influence metal bioavailability (Abeywardhana et al., 2022; Rahman et al., 2024). The present results suggest that species-specific functional responses may complement concentration-based assessments by providing biologically relevant information, especially in systems where sediment geochemistry may exert an important influence on metal behavior.

A key limitation of this study is its temporal resolution, as sampling was conducted during a single campaign in June 2023 and water samples were collected during low tide. Although low-tide conditions were required for field access and seedling collection, water and suspended particulate matter samples collected at this tidal stage do not capture variability across the tidal cycle. The single campaign also does not capture seasonal variation in metal concentrations, partitioning, and biological exposure. While spatial patterns across the contamination gradient are clearly defined, the temporal dynamics of metal uptake, retention, and redistribution remain unresolved. This limitation highlights the importance of temporal monitoring to better understand how these functional responses evolve under changing environmental conditions. Metal availability was inferred from measured metal concentrations in water and sediments, together with sediment geochemical characteristics, rather than directly quantified through chemical speciation analyses. Physiological mechanisms were inferred from accumulation patterns and were not directly validated through biochemical or molecular analyses. Accordingly, the Functional Triad should currently be interpreted as a conceptual framework supported by correlative patterns rather than a mechanistically validated physiological model.

Future studies should prioritize experimental validation of the Functional Triad through: (i) field transplantation and mesocosm experiments to evaluate temporal variation in metal pools; (ii) assessment of metal redistribution dynamics during plant development; (iii) validation of L. *racemosa* translocation patterns as indicators of environmental variability; (iv) evaluation of seedling acclimation processes under environmental stress (Rahman et al., 2024; Yan et al., 2017); (v) seedling-specific toxicity tests to establish effect thresholds for mangrove tissues under environmentally relevant conditions; (vi) investigation of rhizosphere interactions as drivers of metal availability (Dey et al., 2024); and (vii) repeated sampling across tidal stages and use of DGT or passive samplers to improve the characterization of dissolved metal exposure.

In this context, mangrove systems with complementary functional traits provide a useful basis for interpreting patterns of metal exposure within the context of ecosystem functioning. These patterns are consistent with current perspectives on nature-based solutions that integrate ecological processes into environmental management (Rahman et al., 2025; Siregar et al., 2025; Karmakar et al., 2025; Yadav et al., 2023; Al-Solaimani et al., 2022; Hossain et al., 2022). These characteristics make Amazonian mangroves valuable natural laboratories for evaluating environmentally driven shifts in functional metal handling responses.

By integrating geochemical setting, inferred metal availability, and biological responses, the Functional Triad offers a conceptual perspective for interpreting contamination gradients beyond concentration-based assessments. Rather than replacing existing monitoring approaches, this interpretation highlights how species-specific metal handling may complement conventional geochemical assessments and provides a foundation for future studies aimed at evaluating its applicability across tropical mangrove ecosystems. Future validation across different mangrove systems and seasons will be necessary to determine the broader applicability of this conceptual framework.

5. Conclusion

This study shows that assessments based solely on environmental metal concentrations may not fully capture biologically relevant patterns of metal accumulation in Amazonian mangrove ecosystems. The integration of environmental and biological data revealed a spatial mismatch between environmental contamination and species-specific accumulation patterns, highlighting the importance of considering both sediment geochemistry and physiological responses when interpreting contamination gradients. Species-specific functional responses support the use of mangroves as biological indicators, and the Functional Triad provides a conceptual framework linking sediment conditions with biological responses based on correlative patterns rather than a mechanistically validated model. Rather than replacing conventional geochemical assessments, this interpretation provides an additional ecological perspective for understanding contamination dynamics in tropical estuarine systems and establishes a foundation for future studies evaluating its applicability to environmental monitoring. Future temporal monitoring will be necessary to assess how metal accumulation and species-specific responses vary over time.

CRediT authorship contribution statement

Jacyara Nascimento Corrêa: Writing – original draft, Investigation, Formal analysis, Data curation, Conceptualization. **Daniel Richard Lemos Brito:** Methodology, Investigation, Formal analysis. **Ricardo Luvizotto-Santos:** Writing – review & editing, Resources, Methodology, Funding acquisition. **Carlos Eduardo de Rezende:** Writing – review & editing, Supervision, Resources, Methodology, Funding acquisition, Formal analysis. **Marianna Basso Jorge:** Writing – review & editing, Supervision, Resources, Project administration, Methodology, Funding acquisition, Conceptualization.

Funding statement

This work was supported by the Coordination for the Improvement of Higher Education Personnel (CAPES; process No. 88887.675497/2022–00) through a doctoral scholarship awarded to Jacyara

Nascimento Corrêa within the Biodiversity and Biotechnology Network of the Legal Amazon (BIONORTE). Additional financial support for the research mobility at the State University of Northern Rio de Janeiro (UENF), where part of the laboratory analyses were conducted, was provided through CAPES/PROAP (project No. AUXPE-PROAP 2023 no. 88881.895613/2023–01) resources from the BIONORTE Graduate Program. Carlos Eduardo de Rezende is a member of the National Institute of Science and Technology for the Transfer of Materials from Continent to Ocean (INCT-TMC Ocean), supported by the National Council for Scientific and Technological Development (CNPq; grant 405,765/2022–3 and 310,260/2023–0) and the Carlos Chagas Filho Research Support Foundation of the State of Rio de Janeiro (FAPERJ; grant E-26/203.950/2024).

Declaration of competing interest

The authors declare that they have no known competing financial interests or personal relationships that could have appeared to influence the work reported in this paper.

Acknowledgments

The authors thank all colleagues from the Laboratory of Ecotoxicology (LabEcotox, Federal University of Maranhão) for their assistance during field sampling campaigns. We also thank the Environmental Sciences Laboratory (LCA-UENF) for providing access to analytical facilities and technical support during sample preparation and ICP-MS analyses.

Appendix A. Supplementary data

Supplementary data to this article can be found online at https://doi.org/10.1016/j.scitotenv.2026.182350.

Data availability

Data will be made available on request.

References

Abeywardhana, D.C., Adikaram, N.M., Kularatne, R.K.A., 2022. Are mangrove forests reliable sinks of heavy metals due to phytoremediation and other mechanisms? A Sri Lankan perspective. Mar. Pollut. Bull. 177, 113453. https://doi.org/10.1016/j.marpolbul.2022.113453.

Alam, M.R., West, M., Anh Tran, T.K., Stein, T.J., Gaston, T.F., Schreider, M.J., Reid, D. J., MacFarlane, G.R., 2022. Metal(loid) accumulation in the leaves of the grey mangrove (Avicennia marina): assessment of robust sampling requirements and potential use as a bioindicator. Environ. Res. 211, 113065. https://doi.org/10.1016/j.envres.2022.113065.

Alhassan, A.B., Aljahdali, M.O., 2021. Sediment metal contamination, bioavailability, and oxidative stress response in mangrove *Avicennia marina* in Central Red Sea. Front. Environ. Sci. 9, 691257. https://doi.org/10.3389/fenvs.2021.691257.

Aljahdali, M.O., Alhassan, A.B., 2020. Ecological risk assessment of heavy metal contamination in mangrove habitats, using biochemical markers and pollution indices: a case study of *Avicennia marina* L. in the Rabigh lagoon, Red Sea. Saudi J. Biol. Sci. 27, 1174–1184. https://doi.org/10.1016/j.sjbs.2020.02.004.

Al-Solaimani, S.G., Abohassan, R.A., Alamri, D.A., Yang, X., Rinklebe, J., Shaheen, S.M., 2022. Assessing the risk of toxic metals contamination and phytoremediation potential of mangrove in three coastal sites along the Red Sea. Mar. Pollut. Bull. 176, 113412. https://doi.org/10.1016/j.marpolbul.2022.113412.

Arrivabene, H.P., Campos, C.Q., Souza, I.D.C., Wunderlin, D.A., Milanez, C.R.D., Machado, S.R., 2016. Differential bioaccumulation and translocation patterns in three mangrove plants experimentally exposed to iron. Consequences for environmental sensing. Environ. Pollut. 215, 302–313. https://doi.org/10.1016/j.envpol.2016.05.019.

Ashayeri, S.Y., Keshavarzi, B., Moore, F., Ahmadi, A., Hooda, P.S., 2023. Risk assessment, geochemical speciation, and source apportionment of heavy metals in sediments of an urban river draining into a coastal wetland. Mar. Pollut. Bull. 186, 114389. https://doi.org/10.1016/j.marpolbul.2022.114389.

Baker, A.J.M., 1981. Accumulators and excluders-strategies in the response of plants to heavy metals. J. Plant Nutr. 3, 643–654. https://doi.org/10.1080/01904168109362867.

Bakshi, M., Ghosh, S., Chakraborty, D., Hazra, S., Chaudhuri, P., 2018. Assessment of potentially toxic metal (PTM) pollution in mangrove habitats using biochemical markers: a case study on *Avicennia officinalis* L. in and around Sundarban, India. Mar. Pollut. Bull. 133, 157–172. https://doi.org/10.1016/j.marpolbul.2018.05.030.

Bhargava, A., Carmona, F.F., Bhargava, M., Srivastava, S., 2012. Approaches for enhanced metal translocation of heavy metals. J. Environ. Manag. 105, 103–120. https://doi.org/10.1016/j.jenvman.2012.04.002.

Briffa, J., Sinagra, E., Blundell, R., 2020. Heavy metal pollution in the environment and their toxicological effects on humans. Heliyon 6, e04691. https://doi.org/10.1016/j.heliyon.2020.e04691.

Carneiro, L.M., Zucchi, M.R., Jesus, T.B., Silva Júnior, J.B., Hadlich, G.M., 2021. δ13C, δ15N and TOC/TN as indicators of the origin of organic matter in sediment samples from the estuary of a tropical river. Mar. Pollut. Bull. 172, 112857. https://doi.org/10.1016/j.marpolbul.2021.112857.

Carvalho-Neta, R.N.F., Barbosa, G.L., Torres, H.S., Sousa, D.B.P., Castro, J.S., Santos, D. M.S., Tchaicka, L., Almeida, Z.S., Teixeira, E.G., Torres, A.R., 2017. Changes in glutathione S-transferase activity and parental care patterns in a catfish (Pisces, Ariidae) as a biomarker of anthropogenic impact in a Brazilian harbor. Arch. Environ. Contam. Toxicol. 72, 132–141. https://doi.org/10.1007/s00244-016-0326-0.

Carvalho-Neta, R.N.F., Sousa, D.B.P., Macêdo Sobrinho, I.C., Horton, E.Y., Almeida, Z.S., Tchaicka, L., Sousa, A.L., 2019. Biochemical and morphological responses in *Ucides cordatus* (Crustacea, Decapoda) as indicators of contamination status in mangroves and port areas from northern Brazil. Environ. Sci. Pollut. Res. 26, 15884–15893. https://doi.org/10.1007/s11356-019-04849-0.

Chai, M., Li, R., Tam, N.F.Y., Zan, Q., 2019. Effects of mangrove plant species on accumulation of heavy metals in sediment in a heavily polluted mangrove swamp in Pearl River estuary, China. Environ. Geochem. Health 41, 175–189. https://doi.org/10.1007/s10653-018-0107-y.

Chanda, A., Swain, S., Das, S., Seal, A., Ghosh, T., Hazra, S., 2021. Spatial variation of heavy metal accumulation in the sediments adjacent to different mangrove plant species within a mixed mangrove stand. Soil Sediment Contam. 30, 548–568. https://doi.org/10.1080/15320383.2020.1867505.

Chen, J., Yuan, L., Zhang, Y., Xue, J., Yang, B., Wu, H., 2023. Risk assessment of trace metal(loid) pollution in surface water of industrial areas along the Huangpu River and Yangtze River estuary in Shanghai, China. Reg. Stud. Mar. Sci. 57, 102746. https://doi.org/10.1016/j.rsma.2022.102746.

Chowdhury, A., Naz, A., Maiti, S.K., 2023. Distribution, speciation, and bioaccumulation of potentially toxic elements in the grey mangroves at Indian Sundarbans, in relation to vessel movements. Mar. Environ. Res. 189, 106042. https://doi.org/10.1016/j.marenvres.2023.106042.

CONAMA, National Environment Council, 2005. Resolution No. 357, Diário Oficial da União, Brasília, Brazil. Available online: http://conama.mma.gov.br/component/sisconama/?view=atosnormativos.

CONAMA, National Environment Council, 2012. Resolution No. 454, Diário Oficial da União, Brasília, Brazil. Available online: http://conama.mma.gov.br/component/sisconama/?view=atosnormativos.

Corrêa, J.J.M., Cutrim, M.V.J., Cruz, Q.S., 2023. Evaluation of metal contamination in surface sediments and macroalgae in mangrove and port complex ecosystems on the Brazilian equatorial margin. Environ. Monit. Assess. 195, 432. https://doi.org/10.1007/s10661-023-11024-z.

Correa, J.N., Torres, T.A., Brito, D.R.L., Martins, S.E., de Rezende, C.E., Dias, F.J.S., Cutrim, M.V.J., Luvizotto-Santos, R., Jorge, M.B., 2025. Mangrove oysters (*Crassostrea brasiliana*) as biomonitors to assess metal contamination in a macro-tidal estuary on the Amazonian equatorial coast. Quim Nova 48 (5). https://doi.org/10.21577/0100-4042.20250135.

Costa, E.S., Sá, F., Gomes, L.E.O., Silva, C.A., Lima, A.T., Lehrback, B.D., Neto, R.R., 2020. Can severe drought periods increase metal concentrations in mangrove sediments? A case study in eastern Brazil. Sci. Total Environ. 748, 142443. https://doi.org/10.1016/j.scitotenv.2020.142443.

Cutrim, M.V.J., Sá, A.K.D.S., Cruz, Q.S., Azevedo-Cutrim, A.C.G., Santos, R.L., Dias, F.J. S., Jorge, M.B., Cavalcanti-Lima, L.F., 2025. Machine learning assessment of dredging impacts on the phytoplankton community on the Brazilian equatorial margin: a multivariate analysis. Environ. Pollut. 368, 125680. https://doi.org/10.1016/j.envpol.2025.125680.

Das, L., Patel, R., Salvi, H., Kamboj, R.D., 2019. Assessment of natural regeneration of mangrove with reference to edaphic factors and water in southern gulf of Kachchh, Gujarat. India. Heliyon 5, e02250. https://doi.org/10.1016/j.heliyon.2019.e02250.

Delgado, J.F., Lima, L.S., Britto, E.B.C.C., Almeida, M.P., Vieira, K.S., Amorim, R.M., Baptista Neto, J.A., Fonseca, E.M., 2020. Evaluation of metal pollution in sediments and water of Sao Marco Harbor (Maranhão, Brazil). Oceanogr. Fish. Open Access J. 12. https://doi.org/10.19080/ofoaj.2020.12.555837.

Dey, G., Maity, J.P., Banerjee, P., Sharma, R.K., Das, K., Gnanachandrasamy, G., Wang, C.W., Lin, P.Y., Wang, S.L., Chen, C.Y., 2024. Evaluation and mitigation of potentially toxic elements contamination in mangrove ecosystem: insights into phytoremediation and microbial perspective. Mar. Pollut. Bull. 209, 117035. https://doi.org/10.1016/j.marpolbul.2024.117035.

Ding, Qian-Su, Xu, Chao-Qun, Ma, Dong-Na, Wei, Ming-Yue, Gao, Chang-Hao, Zhang, S., Li, Huan, Zhu, ·Xue-Yi, Zheng, Hai-Lei, 2024. Chloride homeostasis via enhanced salt ion secretion selectivity contributes to salt tolerance of recretohalophytic mangrove *Avicennia marina*. Plant Soil 503, 733–750. https://doi.org/10.1007/s11104-024-06619-5.

Donaher, S.E., Estes, S.L., Dunn, R.P., Gonzales, A.K., Powell, B.A., Martinez, N.E., 2024. Site- and species-specific metal concentrations, mobility, and bioavailability in sediment, flora, and fauna of a southeastern United States salt marsh. Sci. Total Environ. 922, 171262. https://doi.org/10.1016/j.scitotenv.2024.171262.

Du, L., Yang, J., He, C., Cui, J., Teng, Z., Chen, Q., 2026. Trace metals in root-stem-leaf of mangrove communities: bioconcentration, migration and biochemical influencing

mechanisms in Circum-Xinying-Bay, Hainan, China. Mar. Pollut. Bull. 231, 119906. https://doi.org/10.1016/j.marpolbul.2026.119906.
El-Sharkawy, M., Alotaibi, M.O., Li, J., Du, D., Mahmoud, E., 2025. Heavy metal pollution in coastal environments: ecological implications and management strategies: a review. Sustainability 17, 701. https://doi.org/10.3390/su17020701.
Guo, Z., Wei, M.Y., Zhong, Y.H., Wu, X., Chi, B.J., Li, J., Li, H., Zhang, L.D., Wang, X.X., Zhu, X.Y., Zheng, H.L., 2023. Leaf sodium homeostasis controlled by salt gland is associated with salt tolerance in mangrove plant Avicennia marina. Tree Physiol. 43, 817–831. https://doi.org/10.1093/treephys/tpad002.
Haydous, F., Nehmeh, B., Rebehmed, J., Al-Alam, J., Saab, C., Sabbagh, S., Hamieh, A., Yassin, A., Wazne, M., Akoury, E., 2025. Unraveling the levels of emerging contaminants along the eastern Mediterranean Sea. Sci. Rep. 15, 4401. https://doi.org/10.1038/s41598-025-89027-8.
Hossain, M.B., Masum, Z., Rahman, M.S., Yu, J., Noman, M.A., Jolly, Y.N., Begum, B.A., Paray, B.A., Arai, T., 2022. Heavy metal accumulation and phytoremediation potentiality of some selected mangrove species from the world's largest mangrove forest. Biol.-Basel 11, 1144. https://doi.org/10.3390/biology11081144.
Hossain, M.S., Ahmed, M.K., Sarker, S., Rahman, M.S., 2020. Seasonal variations of trace metals from water and sediment samples in the northern bay of Bengal. Ecotoxicol. Environ. Saf. 193, 110347. https://doi.org/10.1016/j.ecoenv.2020.110347.
Islam, O., Palash, M.A.I., Akter, M., Kundu, P., Saha, S., Quaraishi, S.B., Hosen, M.M., Khan, S.R., Sarker, A., Xu, Y., Khan, M.F., Uddin, M.K., Baki, M.A., 2026. Transport of metals in surface estuary water, core sediment, roots and leaves of mangrove ecosystem in Bangladesh: bioaccumulation and ecological risk assessment. Mar. Pollut. Bull. 224, 119158. https://doi.org/10.1016/j.marpolbul.2025.119158.
Jatobá-Junior, A.A., Hatje, V., Masque, P., Rezende, C.E., Cabral, A., Yau, Y.Y.Y., Barreira, J., Reithmaier, G.M.S., Santos, I.R., 2025. Carbon and mercury burial in mangrove soils across an anthropogenic gradient. Estuar. Coast. Shelf Sci. 318, 109226. https://doi.org/10.1016/j.ecss.2025.109226.
Jesus, W.B., Mota Andrade, T.S.O., Soares, S.H., Sousa, D.B.P., Oliveira, S.R.S., Torres, H. S., Protazio, G.S., Silva, D.S., Santos, D.M.S., Carvalho-Neta, A.V., Benjamin, L.A., Carvalho-Neta, R.N.F., 2021. Biomarkers and occurrences of heavy metals in sediment and the bioaccumulation of metals in crabs (*Ucides cordatus*) in impacted mangroves on the Amazon coast, Brazil. Chemosphere 271, 129444. https://doi.org/10.1016/J.chemosphere.2020.129444.
Karmakar, S., Riya, K.K., Jolly, Y.N., Akter, S., Mamun, K.M., Kabir, J., Paray, B.A., Arai, T., Yu, J., Ngah, N., Hossain, M.B., 2025. Effectiveness of artificially planted mangroves on remediation of metals released from ship-breaking activities. Mar. Pollut. Bull. 212, 117587. https://doi.org/10.1016/j.marpolbul.2025.117587.
Kumari, P., Pathak, B., 2025. Toxic metal concentration in soil and mangrove plant species across Purna River estuary, gulf of Khambhat, Gujarat. J. Coast. Conserv. 29, 1–21. https://doi.org/10.1007/s11852-024-01095-6.
Lacerda, L.D., Cavalcante, I.B.K., Soares, A.A., Marins, R.V., 2024. Mobility, bioavailability and distribution of Fe and Cu in mangroves (*Avicennia schaueriana* and *Rhizophora mangle*) from a semiarid coast in NE Brazil. An. Acad. Bras. Cienc. 96, e20231075. https://doi.org/10.1590/0001-3765202420231075.
Lacerda, L.D., Rezende, C.E., Aragon, G.T., Ovalle, A.R., 1991. Iron and chromium transport and accumulation in a mangrove ecosystem. Water Air Soil Pollut. 57–58, 513–520. https://doi.org/10.1007/bf00282915.
Lacerda, L.D., Ward, R.D., Borges, R., Ferreira, A.C., 2022. Mangrove trace metal biogeochemistry response to global climate change. Front. For. Glob. Change 5, 817992. https://doi.org/10.3389/ffgc.2022.817992.
Lewis, M., Pryor, R., Wilking, L., 2011. Fate and effects of anthropogenic chemicals in mangrove ecosystems: a review. Environ. Pollut. 159, 2328–2346. https://doi.org/10.1016/j.envpol.2011.04.027.
Li, C., Wang, H., Liao, X., Xiao, R., Liu, K., Bai, J., Li, B., He, Q., 2022. Heavy metal pollution in coastal wetlands: a systematic review of studies globally over the past three decades. J. Hazard. Mater. 424, 127312. https://doi.org/10.1016/j.jhazmat.2021.127312.
Liu, N., Zhao, J., Du, J., Hou, C., Zhou, X., Chen, J., Zhang, Y., 2024. Non-phytoremediation and phytoremediation technologies of integrated remediation for water and soil heavy metal pollution: a comprehensive review. Sci. Total Environ. 948, 174237. https://doi.org/10.1016/j.scitotenv.2024.174237.
Liu, X., Tang, D., Ge, C., 2020. Distribution and sources of organic carbon, nitrogen and their isotopic composition in surface sediments from the southern Yellow Sea, China. Mar. Pollut. Bull. 150, 110716. https://doi.org/10.1016/j.marpolbul.2019.110716.
Long, E.R., MacDonald, D.D., Smith, S.L., Calder, F.D., 1995. Incidence of adverse biological effects within ranges of chemical concentrations in marine and estuarine sediments. Environ. Manag. 19, 81–97. https://doi.org/10.1007/bf02472006.
Macedo, G.H.R.V., Castro, J.S., Jesus, W.B., Torres, H.S., Moreno, L.C.G.A.I., Rosa, R.G., Carvalho-Neta, R.N.F., Sousa, D.B.P., 2024. Biomarkers of oxidative stress in an estuarine catfish species caught near a port complex on the Brazilian Amazon coast. Reg. Stud. Mar. Sci. 69, 103306. https://doi.org/10.1016/j.rsma.2023.103306.
MacFarlane, G.R., Koller, C.E., Blomberg, S.P., 2007. Accumulation and partitioning of heavy metals in mangroves: a synthesis of field-based studies. Chemosphere 69, 1454–1464. https://doi.org/10.1016/j.chemosphere.2007.04.059.
Meyers, P.A., 1997. Organic geochemical proxies of paleoceanographic, paleolimnologic, and paleoclimatic processes. Org. Geochem. 27, 213–250. https://doi.org/10.1016/S0146-6380(97)00049-1.
Mziray, P., Kimirei, I.A., 2024. Metal pollution in mangrove ecosystems in Dar Es Salaam, Tanzania. West. Indian Ocean J. Mar. Sci. 23, 99–113. https://doi.org/10.4314/wiojms.v23i2.8.
Nascimento, L.S., Abreu Pestana, I., Seidel, M., da Silva, Marques, Junior, J., Vaz, Cherene, de Oliveira, B., Ribeiro Gomes, P., Koschinsky, A., Dittmar, T., de Rezende, C.E., 2025. Mercury concentrations along the Amazon estuary and plume: spatial trends and geochemical processes. Environ. Res. 271, 121129. https://doi.org/10.1016/j.envres.2025.121129.
Niu, L., Cai, H., Jia, L., Luo, X., Tao, W., Dong, Y., Yang, Q., 2021. Metal pollution in the Pearl River Estuary and implications for estuary management: the influence of hydrological connectivity associated with estuarine mixing. Ecotoxicol. Environ. Saf. 225, 112747. https://doi.org/10.1016/j.ecoenv.2021.112747.
Nubi, A.O., Popoola, S.O., Dada, O.A., Oyatola, O.O., Unyimadu, J.P., Adekunbi, O.F., Salami, A.M., 2022. Spatial distributions and risk assessment of heavy metals and PAH in the southwestern Nigeria coastal water and estuaries, Gulf of Guinea. J. Afr. Earth Sci. 188, 104472. https://doi.org/10.1016/j.jafrearsci.2022.104472.
NUGEO, Nucleo Geoambiental, 2016. Bacias Hidrográficas e Climatologia do Maranhão. Universidade Estadual do Maranhão, São Luis, Brazil, 166 pp. Available online: https://www.nugeo.uema.br/upnugeo/publicacoes/Bacias%20Hidrogr%C3%A1ficas%20e%20Climatologia%20-%20MA.
Pestana, I.A., Bastos, W.R., Almeida, M.G., Mussy, M.H., Souza, C.M., 2019. Methylmercury in environmental compartments of a hydroelectric reservoir in the Western Amazon, Brazil. Chemosphere 215, 758–765. https://doi.org/10.1016/j.chemosphere.2018.10.106.
Rahman, S.U., Han, J.C., Yasin, G., Shah, A.M., 2025. Meta-analysis of mangrove phytoremediation for heavy metal mitigation in coastal regions of China. Ecol. Eng. 219, 107683. https://doi.org/10.1016/j.ecoleng.2025.107683.
Rahman, S.U., Han, J.C., Zhou, Y., Ahmad, M., Li, B., Wang, Y., Huang, Y., Yasin, G., Ansari, M.J., Saeed, M., Ahmad, I., 2024. Adaptation and remediation strategies of mangroves against heavy metal contamination in global coastal ecosystems: a review. J. Clean. Prod. 441, 140868. https://doi.org/10.1016/j.jclepro.2024.140868.
Rezaei, M., Kafaei, R., Mahmoodi, M., Sanati, A.M., Vakilabadi, D.R., Arfaeinia, H., Dobaradaran, S., Sorial, G.A., Ramavandi, B., Boffito, D.C., 2021. Heavy metals concentration in mangrove tissues and associated sediments and seawater from the north coast of Persian gulf, Iran: ecological and health risk assessment. Environ. Nanotechnol. Monit. Manage. 15, 100456. https://doi.org/10.1016/j.enmm.2021.100456.
Rezende, C.E., Lacerda, L.D., Ovall, A.R.C., Silva, C.A.R., Martinelli, L.A., 1990. Nature of POC transport in a mangrove ecosystem: a carbon stable isotopic study. Estuar. Coast. Shelf Sci. 30, 641–645. https://doi.org/10.1016/0272-7714(90)90099-d.
Righi, B.D.P., Abujamara, L.D., Barcarolli, I.F., Jorge, M.B., Zebral, Y.D., Costa, P.G., Martinez, C.B.R., Bianchini, A., 2022. Response of biomarkers to metals, hydrocarbons and organochlorine pesticides contamination in crabs (*Callinectes ornatus* and *C. bocourti*) from two tropical estuaries (São José and São Marcos bays) of the Maranhão State (northeastern Brazil). Chemosphere 288, 132649. https://doi.org/10.1016/j.chemosphere.2021.132649.
Santos, V.H.M., Dias, F.J.S., Torres, A.R., Soares, R.A., Terto, L.C., Castro, A.C.L., Santos, R.L., Cutrim, M.V.J., 2020. Hydrodynamics and suspended particulate matter retention in macrotidal estuaries located in Amazonia-semiarid interface (northeastern-Brazil). Int. J. Sediment Res. 35, 417–429. https://doi.org/10.1016/j.ijsrc.2020.03.004.
Sartori, É., Vergilio, C.S., Gatts, P.V., Oliveira, B.C.V., Almeida, M.G., Thompson, F., Rezende, C.E., 2023. Trace metal concentration along the Brazilian coast: an assessment of the influence of the Doce River plume. Mar. Pollut. Bull. 188, 114640. https://doi.org/10.1016/j.marpolbul.2023.114640.
Silva, M.H.L., Castro, A.C.L., Silva, I.S., Cabral, P.F.P., Azevedo, J.W.J., Soares, L.S., Bandeira, A.M., Basso, M.J., Nunes, J.L.S., 2023. Determination of metals in estuarine fishes in a metropolitan region of the coastal zone of the Brazilian Amazon. Mar. Pollut. Bull. 186, 114477. https://doi.org/10.1016/j.marpolbul.2022.114477.
Siregar, E.S., Jumilawaty, E., Tanjung, M., Syafitri, A., Kusmana, C., Basyuni, M., Hartanto, A., Rahmania, R., 2025. Bioaccumulation of heavy metals by Acanthus ilicifolius in polluted mangrove. Emerg. Sci. J. 9, 557–568. https://doi.org/10.28991/esj-2025-09-02-03.
Souza Filho, P.W.M., 2005. Costa de manguezais de macromaré da Amazônia: cenários morfológicos, mapeamento e quantificação de áreas usando dados de sensores remotos. Rev. Bras. Geofis. 23, 427–435. https://doi.org/10.1590/s0102-261x2005000400006.
Sreelekshmi, S., Harikrishnan, M., Nandan, S.B., Sreelakshmi, M.N., Philomina, J., Neethu, K.V., 2022. Ecological risk assessment and phytomanagement of trace metals in the sediments of mangroves associated with the Ramsar sites of Kerala, southern India. Environ. Sci. Pollut. Res. 30, 30530–30547. https://doi.org/10.1007/s11356-022-24375-w.
Suman, J., Uhlik, O., Viktorova, J., Macek, T., 2018. Metal translocation of heavy metals: a promising tool for clean-up of polluted environment? Front. Plant Sci. 871, 392782. https://doi.org/10.3389/fpls.2018.01476.
Szafranski, G.T., Granek, E.F., 2023. Contamination in mangrove ecosystems: a synthesis of literature reviews across multiple contaminant categories. Mar. Pollut. Bull. 196, 115595. https://doi.org/10.1016/j.marpolbul.2023.115595.
Thanh-Nho, N., Strady, E., Nhu-Trang, T.T., David, F., Marchand, C., 2018. Trace metals partitioning between particulate and dissolved phases along a tropical mangrove estuary (can Gio, Vietnam). Chemosphere 196, 311–322. https://doi.org/10.1016/j.chemosphere.2017.12.189.
U.S. Environmental Protection Agency (EPA), 1996. Method 3052: Microwave Assisted Acid Digestion of Siliceous and Organically Based Matrices. . SW-846 Test Methods for Evaluating Solid Waste, Physical/Chemical Methods.
U.S. Environmental Protection Agency (EPA), 2007. Method 3015A: Microwave Assisted Acid Digestion of Aqueous Samples and Extracts. . SW-846 Test Methods for Evaluating Solid Waste, Physical/Chemical Methods, Revision 1.
Usman, A.R.A., Alkredaa, R.S., Al-Wabel, M.I., 2013. Heavy metal contamination in sediments and mangroves from the coast of Red Sea: Avicennia marina as potential

metal bioaccumulator. Ecotoxicol. Environ. Saf. 97, 263–270. https://doi.org/10.1016/j.ecoenv.2013.08.009.

Yadav, K.K., Gupta, N., Prasad, S., Malav, L.C., Bhutto, J.K., Ahmad, A., Gacem, A., Jeon, B.H., Fallatah, A.M., Asghar, B.H., Cabral-Pinto, M.M.S., Awwad, N.S., Alharbi, O.K.R., Alam, M., Chaiprapat, S., 2023. An eco-sustainable approach towards heavy metals remediation by mangroves from the coastal environment: a critical review. Mar. Pollut. Bull. 188, 114569. https://doi.org/10.1016/j.marpolbul.2022.114569.

Yadav, V.B., Pulhani, V.A., Kumar, A.V., 2025. Study of sedimentary organic carbon using δ13C, δ15N and TOC/TN as indicator in sediment core samples from Mumbai Harbor bay. Environ. Monit. Assess. 197, 1–17. https://doi.org/10.1007/s10661-025-13980-0.

Yan, Z., Sun, X., Xu, Y., Zhang, Q., Li, X., 2017. Accumulation and tolerance of mangroves to heavy metals: a review. Curr. Pollut. Rep. 3, 302–317. https://doi.org/10.1007/s40726-017-0066-4.

Zhang, M., Liu, C., Zhang, C., Zhu, H., Wan, J., Liu, X., 2023. Response of macrofaunal assemblages to different pollution pressures of two types of ports. Ecol. Indic. 146, 109858. https://doi.org/10.1016/j.ecolind.2022.109858.

Zhou, W., Cao, Q., Hong, M., Lei, Y., Wen, D., Zhang, D., 2022. Spatial distribution and risk assessment of heavy metals in seawater and sediments in Jieshi Bay, Shanwei, China. Front. Mar. Sci. 9, 1011564. https://doi.org/10.3389/fmars.2022.1011564.